



Mineralogical and environmental effects on the $\delta^{13}\text{C}$, $\delta^{18}\text{O}$, and clumped isotope composition of modern bryozoans

Marie Pesnin ^{a,*}, Caroline Thaler ^{a,b}, Mathieu Daëron ^a, Sébastien Nomade ^a, Claire Rollion-Bard ^a

^a Laboratoire des Sciences du Climat et de l'Environnement (LSCE), CNRS, CEA, UVSQ, Université Paris-Saclay, Gif-sur-Yvette 91191, France

^b Bloomineral, French SAS, 5 Terrasse des reflets, Courbevoie 92400, France



ARTICLE INFO

Editor: Dr. Vasileios Mavromatis

Keywords:

Bryozoan
Clumped isotopes
Isotopic disequilibrium
Paleoclimate reconstructions

ABSTRACT

Extensive bryozoan fossil records date back to the early Ordovician, forming an important part of sedimentary archives, yet the applicability of classical 18-oxygen thermometry to bryozoan carbonate is still a matter of debate, with mineralogical and biological issues still hindering paleoclimate reconstructions. Complementing other methods (i.e., $\delta^{18}\text{O}$, Mg/Ca), clumped-isotope thermometry (Δ_{47}) could provide more accurate paleotemperature estimates and help identify potential biotic factors influencing the isotopic composition of bryozoans. Here we report on the first investigation of clumped-isotope thermometry applied to bryozoan carbonate, spanning a broad range of modern species living in different environments from two localities (Atlantic Ocean and Mediterranean Sea). We confirm that bryozoan $\delta^{13}\text{C}$ and $\delta^{18}\text{O}$ records are affected by biotic and abiotic factors susceptible to bias in growth condition estimates. Our Atlantic bryozoans yield Δ_{47} derived temperatures (T_{47}) consistent with spring/fall seawater temperature (but only after correcting for minor mineralogical effects), reflecting seasonal growth bias or, more likely, moderate isotopic disequilibrium. By contrast, Mediterranean samples display large positive offsets from Δ_{47} equilibrium values. We propose that this stronger disequilibrium is related to the higher salinity at this site, decreasing Carbonic Anhydrase activity, favoring CO₂ hydroxylation over hydration, and slowing down DIC (dissolved inorganic carbon) equilibration reactions at the precipitation site. Our findings highlight how "vital effects" in bryozoans is not only species-specific as often assumed for other biocalcifiers, but could also depend on mineralogy and environmental factors.

1. Introduction

Biologists have long described bryozoans as a minor phylum, probably because of their small size and the difficulty of identifying them (Smith, 2014). This taxon remains therefore less scrutinized than mollusks or cnidarians. Nevertheless, the extensive fossil record and remarkable shape diversity of bryozoans have long attracted the interest of paleontologists. Bryozoans are sessile colonial epibionts formed from clonal individuals called zooids, with morphologies ranging from encrusting to erect (Smith, 2014). About 20,000 species of bryozoans are known, 5896 of which remain extant (Taylor et al., 2010; Taylor and Waeschenbach, 2015), with the oldest forms dating back to the Ordovician (Taylor and Kuklinski, 2011). Since their appearance they have

colonized all aquatic environments, from freshwater lakes to marine abyssal plains, including continental shelves where they are ubiquitous, making them one of the most common phyla found in carbonate platform archives. All freshwater bryozoans have soft skeletons, but many marine bryozoans build a calcareous skeleton and, like corals, play an important role in supporting marine ecosystems. Bryozoan colonies can grow over several years, even decades (Cocito et al., 1998; Brey et al., 1999; Bader and Schäfer, 2005). Carbonate production in short-lived ones (< 10 years) ranges between 10^{-1} to 10^{-2} mg.y⁻¹ (Smith, 2014), while long-lived species could reach 23.7 mg.y⁻¹ (Smith et al., 2001). It was noticed that bryozoans' growth rate varies seasonally over the course of a year, coldest periods (from late autumn to early spring) being marked by reduced or even no growth, while warmer periods are

* Corresponding author.

E-mail address: mariepesnin@outlook.com (M. Pesnin).

characterized by enhanced skeleton growth (Stebbing, 1971; Ryland and Sykes, 1972; Cocco et al., 1998; Fortunato, 2015). Thus, interannual variations in bryozoan chemistry are more likely to represent changes in seawater properties during warmer months of the year.

Although bryozoans are among the most important benthic carbonate producers of non-tropical continental shelves, our knowledge on their calcification process is less extensive than for other calcifiers. Most studies on this subject have focused on their mineralogical composition and its evolution through the geological record. Bryozoans have the ability to build a hard skeleton comprising different calcium carbonate polymorphs (Fortunato, 2015; Taylor et al., 2015). They can be entirely aragonitic (15%), entirely calcitic or Mg-calcitic (65%) or bimimetic (20%) (Lombardi et al., 2008). Given their pluri-mineralogic characteristics, numerous studies have attempted to understand the links between chemical/physical changes (e.g., pH, saturation state, temperature) and temporal variations in bryozoan mineralogy (Smith et al., 2006; Lombardi et al., 2008; Taylor et al., 2009; Loxton et al., 2014; Smith, 2014; Swezey et al., 2017; Figuerola et al., 2023). Morphological changes within bryozoan colonies were also investigated, which led to propose a relationship between zooid size and seasonal variations in water chemistry, forming the basis of the MART (Mean Annual Range of Temperature) method (O'Dea, 2003; Smith and Key, 2004; Knowles et al., 2009). Although temperature appears to be the main driver for most of the observed variations in zooid size (Amui-Vedel et al., 2007; Hageman et al., 2009; Knowles et al., 2010), some studies reported contradictory results supported by geochemical data (Jackson and Herrera-Cubilla, 2000; Novosel et al., 2004; Berning et al., 2005), casting doubts on the ability of this proxy to provide reliable temperature reconstructions. On the other hand, few researchers have attempted thus far to use bryozoan stable isotopes ($\delta^{18}\text{O}$ and $\delta^{13}\text{C}$) or elemental ratios for paleoenvironmental applications (Forester et al., 1973; Rao and Nelson, 1992; Machiyama et al., 2003). Very little is known about isotopic fractionation between bryozoan skeleton and water or Dissolved Inorganic Carbon (DIC). Additionally, the fact that their skeleton can comprise more than one calcium carbonate polymorph further complicates interpretations. The few studies attempting to address the issue, by comparing modern bryozoan $\delta^{18}\text{O}$ and $\delta^{13}\text{C}$ to monitored environmental parameters (Brey et al., 1999; Crowley and Taylor, 2000; Smith et al., 2004) or ancient bryozoan isotopic record to other biocalcifiers (Håkansson and Madsen, 1991; Key Jr et al., 2005) obtained contradictory results supporting the existence of potential vital effects on bryozoan carbon and oxygen isotopic compositions.

Here we attempt to shed some light on these issues by systematically investigating the mineralogical, elemental (Mg/Ca and Sr/Ca), stable isotope ($\delta^{13}\text{C}$, $\delta^{18}\text{O}$) and “clumped-isotope” signatures in nine modern bryozoan species.

Regarding clumped-isotope, the Δ_{47} anomaly/tracer denotes the statistical overabundance of ^{13}C - ^{18}O bonds within the carbonate mineral (Eiler and Schauble, 2004; Schauble et al., 2006). For fundamental reasons, Δ_{47} values at thermodynamic equilibrium are expected to decrease as equilibration temperature increases, potentially constraining crystallization temperatures (Ghosh et al., 2006). In contrast to more traditional approaches such as $\delta^{18}\text{O}$ or Mg/Ca thermometry, clumped-isotope thermometry does not require any knowledge of the seawater composition ($\delta^{18}\text{O}_{\text{sw}}$, Mg/Ca_{sw}), making it possible to independently constrain both seawater temperature and $\delta^{18}\text{O}_{\text{sw}}$ from combined Δ_{47} and $\delta^{18}\text{O}$ measurements. Over the past 15 years, Δ_{47} signatures has been documented in wide variety of biocarbonates including foraminifera (Tripati et al., 2010; Peral et al., 2018; Meinicke et al., 2020), bivalves (Henkes et al., 2013; Huyghe et al., 2022; De Winter et al., 2022), cephalopods (Davies et al., 2021), echinoderms

(Davies and John, 2019), corals (Thiagarajan et al., 2011; Saenger et al., 2012; Spooner et al., 2016; Kimball et al., 2016), brachiopods (Henkes et al., 2013; Bajnai et al., 2018; Davies et al., 2023), freshwater ostracods (Marchegiano et al., 2024), land snails (Dong et al., 2021). Although certain organisms, such as corals, echinoderms or brachiopods, are now known to present large departures from equilibrium Δ_{47} values (e.g., Saenger et al., 2012; Bajnai et al., 2018; Davies et al., 2021), many other carbonates, both biogenic and abiotic, appear to follow the same equilibrium relationship between Δ_{47} and formation temperature, despite being formed under very diverse chemical conditions (Daëron and Vermeesch, 2024, and references therein).

In cases where ^{13}C - ^{18}O bonds do not attain an equilibrium distribution, clumped-isotopes may nevertheless be used to investigate biomineralization processes and potentially correct isotopic disequilibrium effects (e.g., Bajnai et al., 2020; Fiebig et al., 2021; Davies et al., 2022, 2023). Recent developments in isotope exchange modeling suggest that clumped-isotope may capture the key processes governing equilibrium and disequilibrium fractionations (Uchikawa et al., 2021; Guo, 2020; Watkins and Devriendt, 2022). These frameworks open new perspectives for studying the interactions between biotic (growth rate, cellular activity, enzymatic activity) and abiotic (pH, T, Salinity, [DIC], pCO₂) factors controlling kinetic isotope effects (KIEs) involved in the formation of carbonates. In the context of bryozoans, these new approaches would be particularly helpful to better understand the evolution of calcification patterns within the Bryozoa phylum and through time.

In order to distinguish biotic from abiotic factors controlling bryozoan isotopic record, we compared the isotopic compositions ($\delta^{18}\text{O}$, $\delta^{13}\text{C}$, Δ_{47}) between different bryozoan species from the same locality/environmental conditions on one hand, and of a bryozoan colony of the same species from two different localities. To quantify potential vital effects, the observed isotopic signatures were systematically compared to values expected from empirical calibrations (e.g., Tarutani et al., 1969; Kim et al., 2007b; Daëron and Vermeesch, 2024) based on in situ environmental data (temperature, pH, salinity, and $\delta^{13}\text{C}_{\text{DIC}}$). Finally, we constrain potential mineralogical effects on stable and clumped-isotope fractionations by systematically comparing isotopic compositions with the mineralogy (Aragonite, Calcite, Mg-calcite) and elemental content (Mg and Sr) of the bryozoan skeleton.

2. Materials

2.1. Sampling sites and bryozoan collection

In order to investigate the stable and clumped-isotope fractionation between water and marine bryozoan skeletons, we selected only living bryozoan species for which physico-chemical parameters of seawater were monitored. Live bryozoan colonies were collected in June 2019 from localities where SOMLIT stations (Service d'Observation en Milieu Littoral) provide weekly records of seawater temperature, salinity and pH. Two sites with distinct environmental parameters were selected: Roscoff and Banyuls (Table 1). Bryozoans from Roscoff were collected in the Northern English Channel directly on the SOMLIT-Astan station (48°46'40 N, 3°56'15 W) at 11 m and 23 m depth and those from Banyuls, in the North-Western Mediterranean Sea a few meters away from the SOMLIT-Sola (42°29'300 N, 03°08'700 E) station, at 27 m depth (Fig. 1a). Fig. 1b and c show the seasonal variability of temperature and salinity at the two sites. Temperature and salinity measurements were carried out weekly using a rosette CTD system (conductivity, temperature, depth) at the sub-surface (11 m) and at the bottom (23 m) of the SOMLIT-Astan station and directly at the depth (27 m) of the SOMLIT-Sola station. Seawater pH (total scale) was weekly measured between

Table 1
Physicochemical parameters of seawater together with carbon and oxygen isotope compositions of DIC and water, respectively at the sampling sites. Uncertainties includes 1SD around calculated average (Temperature, Salinity, pH and $\delta^{18}\text{O}_{\text{sw}}$).

Collection locality	Water depth (m)	Temperature (°C)	Salinity (psu)		pH	$\delta^{18}\text{O}_{\text{sw}}^*$ (‰)		$\delta^{13}\text{C}_{\text{DIC}}^{**}$ (‰)		
						Annual average	Growth period			
			Annual average	Growth period						
Roscoff (Astan)	23	12.92 ± 1.80	13.87 ± 1.47	35.2 ± 0.1	7.84 ± 0.1	7.84 ± 0.1	0.44 ± 0.02	1.5 ± 0.5		
Roscoff (Astan)	11	12.93 ± 1.80	13.87 ± 1.47	35.2 ± 0.1	7.84 ± 0.1	7.84 ± 0.1	0.44 ± 0.02	1.5 ± 0.5		
Banyuls (Sola)	24	15.31 ± 2.72	16.34 ± 2.50	38.1 ± 0.3	8.03 ± 0.3	8.04 ± 0.14	1.32 ± 0.08	1.34 ± 0.08		

* $\delta^{18}\text{O}_{\text{sw}}$ values based on the salinity and Lartaud et al. (2010) calibration at Roscoff and Pierre (1999) calibration at Banyuls.
 ** $\delta^{13}\text{C}_{\text{DIC}}$ estimated from the global gridded dataset of Liu et al. (2021).

0 and 30 m depth at both stations using a spectrophotometric approach with m-cresol purple (Douglas and Byrne. 2017). Temperature, salinity and pH records from 1997 onwards are accessible from SOMLIT web site (www.somlit.fr). We did not directly measure the $\delta^{18}\text{O}$ of the water and $\delta^{13}\text{C}$ of the DIC in this study. The $\delta^{18}\text{O}_{\text{sw}}$ values at each site were estimated from salinity records based on regional transfer equations (Lartaud et al., 2010, for the French Atlantic Ocean; Pierre, 1999, for the Mediterranean Sea). These reconstructed $\delta^{18}\text{O}_{\text{sw}}$ values (Table 1) are in good agreement with those derived from the global gridded Atlas of LeGrande and Schmidt (2006). The $\delta^{13}\text{C}$ values of the DIC at each site were estimated based on the global gridded dataset of Liu et al. (2021) (Table 1). Like most coastal bio-calcifiers, bryozoan skeleton growth is seasonal (Stebbing, 1971; Ryland and Sykes, 1972; Cocito et al., 1998). From late autumn to early spring, when nutrient levels and temperature are at their lowest, bryozoans almost entirely stop their growth to reduce energy consumption (Fortunato, 2015). Thus, the composition of our samples is expected to record environmental conditions from springs to early autumns in the year preceding our sampling (June to October 2018 and April to June 2019).

2.2. Sampling strategy and cleaning procedures

In total, three bryozoan species from Banyuls and seven from Roscoff, including one species in common to both sites (*Pentapora foliacea*) were collected (Table 2). Immediately after collection, all samples were rinsed in deionized water to remove any salt residue, then dried at ambient temperature. For all bryozoan species, the most recent part of each skeleton corresponding to one year of growth (i.e., the tips) was detached from the rest of the colony. Branching colonies such as *Cellaria fistulosa*, *Crisia denticulata*, *Cellepora pumicosa* or *Osmalosecosa ramulosa* typically build one new branch at the top of their skeleton each year (Tavener-Smith and Williams, 1972). We, thus sampled these newly formed branches at the top of the colony (tips) measuring about ~1 cm long each for analysis (Fig. 2, e, f, g). Several tips per colony were sampled in order to avoid biases linked to intra-colony heterogeneities (Smith and Key, 2004, Supplementary Material Fig. A.4, A.6). Massive colonies such as *P. foliacea* sometimes exhibit well-developed growth marks such as alternating dark and clear growth bands (Stebbing, 1971). The last year of growth corresponding to a thinner and clearer layer surrounding a dark line in the skeleton is thus easily identified (Lombardi et al., 2006). We collected up to three pieces, each around 10 by 5 mm, from the uppermost part of the colonies for chemical characterization (Fig. 2, a, b, c, d). *Membranipora membranacea*, *Sertella beaniana*, *Tubicellepora avicularis* are also part of massive bryozoan colonies group. However, all of them did not show well developed growth mark. We thus based our sampling on the assumption that 1 year of growth would represent about 1 cm length as described in previous studies (Cocito et al., 1998; Fortunato, 2015). Finally, in order to assess intra-colony changes, we also collected three samples from the base of the colony (the oldest part of the colony attached to the substrate) from the massive species of *P. foliacea*.

Before performing isotopic measurements, we tested different cleaning procedures and evaluated their potential effect on the calcium carbonate isotopic signatures, i.e., $\delta^{18}\text{O}$, $\delta^{13}\text{C}$ and Δ_{47} . One of these cleaning procedures implies an oxidative stage (Supplementary Material, protocols 4, 5, 6, 7), whereas the other does not (Supplementary Material, protocols 1, 2, 3). These two cleaning procedures were tested on *C. fistulosa* and *P. foliacea* bryozoan species, because of their differences in shape and in mineralogy. Both cleaning procedures require a first step of rinsing in de-ionized water neutralized at pH above 7 with NaOH (0.1 M) solution. We have taken the precaution to perform very short sonication cycles of 30 s during this first step to avoid any potential loss of mineralogical features in our samples (Loxton et al., 2017), while improving salt and organic matter removal. This first step was repeated twice for all samples. Samples were then rinsed one last time with neutralized de-ionized water over a 0.2 μm nylon filter mounted on a

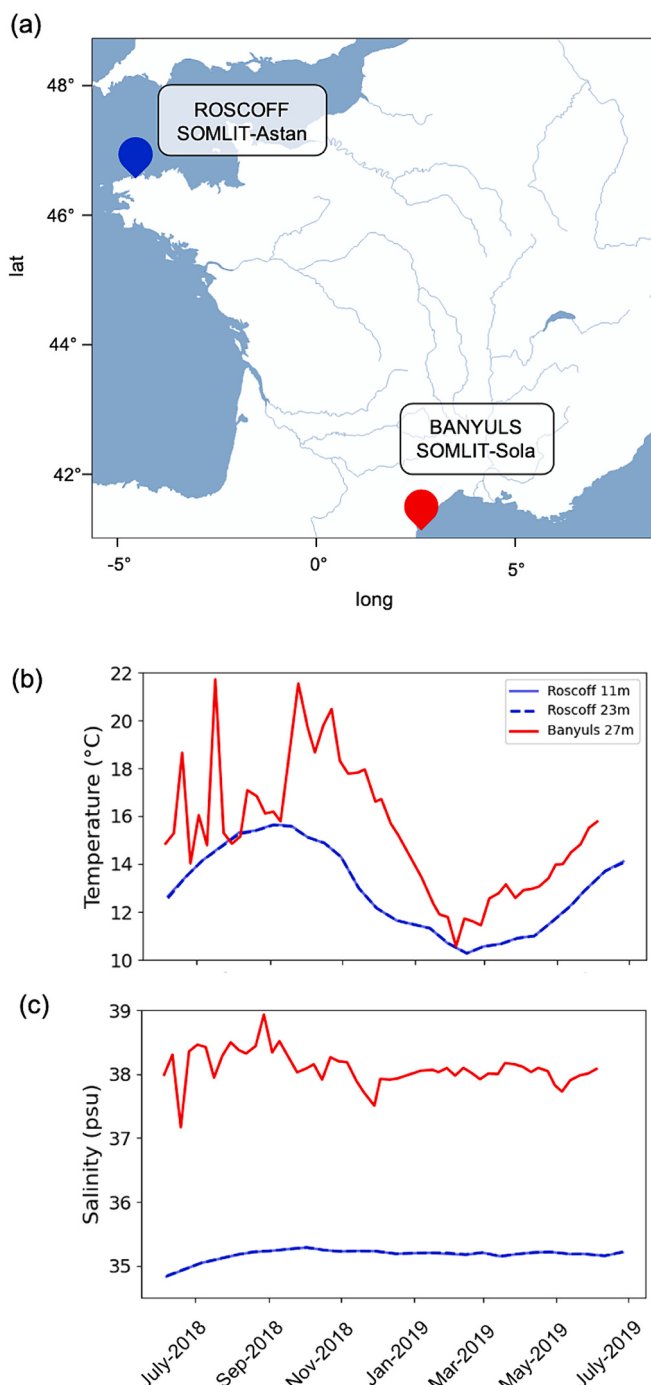


Fig. 1. (a) Location of the two sampling sites accompanied by weekly record of (b) temperature and (c) salinity measured at the SOMLIT stations Astan (blue) and Sola (red) between June 2018 and June 2019. No difference is observed between the temperature and the salinity recorded at 11 m and 23 m depth at Roscoff and the two curves are superimposed. (For interpretation of the references to colour in this figure legend, the reader is referred to the web version of this article.)

vacuum filtration unit, and dried at room temperature in a drying oven under vacuum. In order to test the effect of organic matter removal on the isotopic compositions, half of the dried samples was recovered for a second cleaning step in which they were rinsed in an oxidative solution composed of NaOH (0.5 M) + H₂O₂ (15%) at 40 °C for 30 min, before being rinsed and dried another time as described above. We tested these two cleaning procedures on entire pieces (0.5 cm², Supplementary

Table 2

Order, species, collection locality, water depth of the collection and bryozoan sampling details.

Order	Species	Collection locality	Water depth (m)	Samples part of the colony
Cheilostomata	<i>Pentapora foliacea</i>	Roscoff	23	Tips
Cheilostomata	<i>Pentapora foliacea</i>	Roscoff	23	Base
Cyclostomata	<i>Crisia denticulata</i>	Roscoff	23	Tips
Cheilostomata	<i>Cellepora pumicosa</i>	Roscoff	23	Tips
Cheilostomata	<i>Osmalosecosa ramosula</i>	Roscoff	23	Tips
Cheilostomata	<i>Cellaria fistulosa</i>	Roscoff	23	Tips
Cheilostomata	<i>Membranipora membranacea</i>	Roscoff	11	Tips
Cheilostomata	<i>Sertella beaniana</i>	Banyuls	27	Tips
Cheilostomata	<i>Pentapora foliacea</i>	Banyuls	27	Tips
Cheilostomata	<i>Tubicellepora avicularis</i>	Banyuls	27	Tips

Material, protocols 1, 4, 7), coarse-grained powder (> 350 µm, Supplementary Material, protocols 2, 5) and fine-grained powder (> 250 µm, Supplementary Material, protocols 3, 6). Finally, we also tested the effect of a last rinse with methanol to improve sample drying and organic matter removal by flocculation (Supplementary Material, protocols 2b, 2c, 4b, 4c, 5b, 5c). After drying all samples were finely crushed and homogenized. Results are presented in Supplementary Material. Table A.1. No significant differences in Δ_{47} values at the 0.01‰ level were detected between the cleaning procedures (see Supplementary Material. Fig. A.4, A.5, A.6 for details). The maximum differences observed for $\delta^{13}\text{C}$ and $\delta^{18}\text{O}$ between cleaning treatments are about 0.95 ‰ and 0.47 ‰, respectively, and can most likely be attributed to intra-colony isotopic variability. Regardless of fragment size, nearly all samples submitted to an oxidative pretreatment yield lower $\delta^{18}\text{O}$ and $\delta^{13}\text{C}$ values. Similar effects of H₂O₂ pretreatment were previously observed in other biocarbonates such as corals, foraminifera, or coralline algae, and have been interpreted as potentially reflecting preferential dissolution of isotopically enriched part of calcium carbonate during the oxidative cleaning step (Grottoli et al., 2005; Peral et al., 2018; Key Jr et al., 2020). Based on our observations and other studies alerting on the effect of oxidative treatment on stable isotope composition of calcium carbonate samples (Boiseau and Juillet-Leclerc, 1997; Lebeau et al., 2014; Key Jr et al., 2020), we opted to forego this potentially destructive oxidative step and cleaned all samples with the following procedure: We first crushed the samples to coarse powder then rinsed the powder twice in neutralized de-ionized water and finally dried the samples under vacuum at room temperature for 48 h. (see Supplementary Material. Fig. A.2).

3. Analytical methods

3.1. X-Ray powder Diffraction (XRD)

The mineralogical content of our bryozoan samples was characterized using X-Ray powder Diffraction (XRD). XRD measurement was obtained on 100 mg calcium powder of each bryozoan species. To obtain this 100 mg powder several tips of the same colony were crushed together and homogenized so that XRD results take into account the natural variability in term of mineralogical content of the bryozoan skeleton. XRD analyses were performed using a Panalytical Empyrean diffractometer equipped with a Cu anode ($\lambda\text{K}\alpha = 1.541874 \text{ \AA}$) and a multichannel X'celerator detector allowing to access to the content of aragonite, calcite and Mg-calcite (Supplementary data 4). Mg-calcite produces distinct XRD spectrum from calcite related to change in the crystal lattice due to Mg substitution to Ca and easily to detect in bryozoan. An example of how the difference between the two spectra is marked in bryozoan samples is given in Fig. B5 of Supplementary data 1.

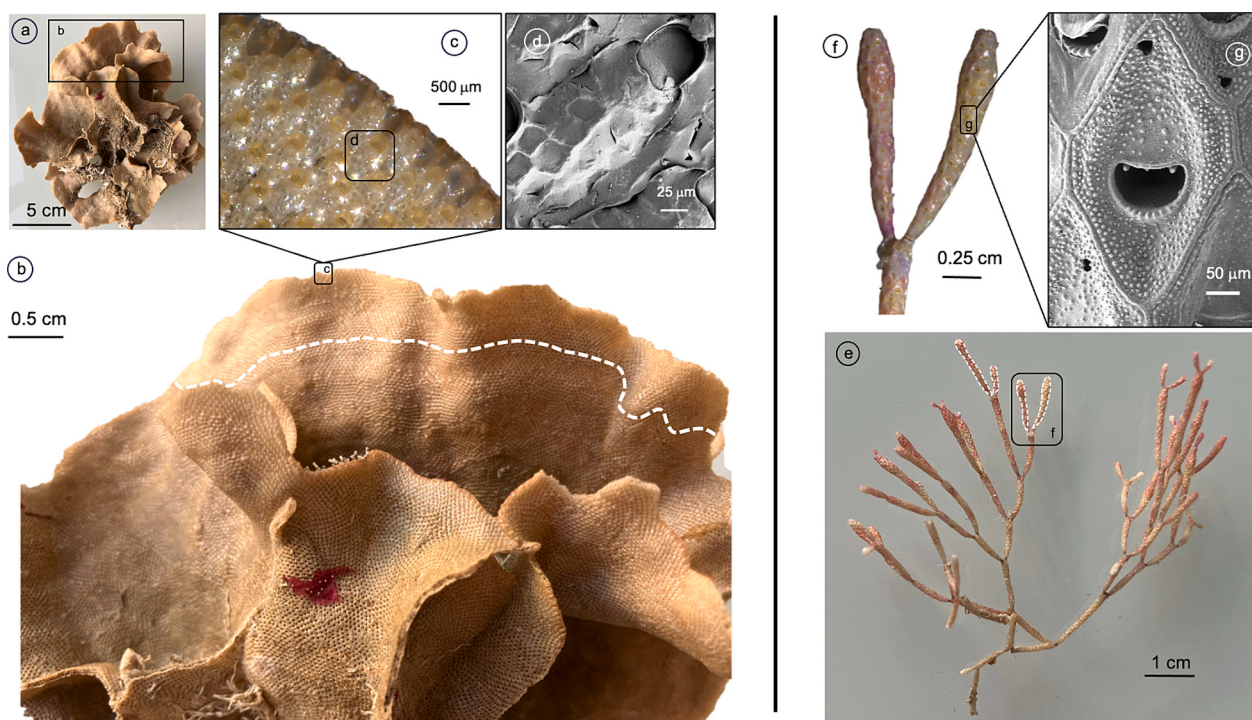


Fig. 2. Sampling strategy for massive (*P. foliacea*: a, b, c, d) and branching (*C. fistulosa*: e, f, g) bryozoan colonies. General view of a dried uncleansed *P. foliacea* (a) and *C. fistulosa* (e) whole colony. (b), (f) Zoom on the last growing part i.e., tips of the colony, which was sampled for isotopic and elemental analysis. The dashed white line symbolizes the limit between the last year of growth and the rest of the skeleton. (c) Zoecium chamber arrangement within the *P. foliacea* colony observed under a binocular magnifier (Leica, DMS 1000). (d), (g) Structure of a single zoecium chamber observed under scanning electron microscope (SEM).

Each pattern was recorded during 60s each 0.0131° in the 0-0 Bragg-Brentano geometry (10°- 65° 2θ range). The detection limit was estimated to be around 0.5%. Mineral identification was performed using the Highscore Plus 3.0 software and two databases: ICSD (Inorganic Crystal Structure Database) and COD (Crystallography Open Database). We have chosen the Rietveld method (Lutterotti et al., 2004) to analyze the whole diffraction pattern. The MAUD program (Material Analysis Using Diffraction) is a general diffraction program mainly based on the Rietveld method and specially used for quantitative phase analysis and refinement of lattice parameters in this work. For samples containing N mineralogical phases (as it is the case for bryozoans), quantitative phase determination using the Rietveld method only provides errors on N-1 phases. In our case, the XRD spectrum of Mg-calcite was taken as the reference for this calculation, and errors are then calculated only for the aragonite and calcite phases (Table 3, Supplementary data 4).

3.2. Stable and clumped-isotope measurements

A total of 332 clumped-isotope analyses (153 sample analyses and 179 reference materials), were performed over 10 analytical sessions between 2022 and 2023 at LSCE's clumped-isotope facility. For each analysis, 3.5–4.0 mg of carbonate powder were converted to CO₂ by reaction with 103% phosphoric acid at 90 °C in a common acid bath for 10 min. Residual water was cryogenically removed from the product CO₂, which was then flushed with Helium (25 mL/min) through a Porapak Q column held at –20 °C and quantitatively recollected by cryogenic trapping. Final CO₂ pressure at room temperature (20 °C) was then directly measured within a small cold finger volume to estimate the CO₂ yield for each acid reaction based on the CO₂ yield for pure CaCO₃ standards (ETH-1/2/4). The CO₂ was then transferred into an Isoprime 100 dual-inlet mass spectrometer equipped with 6 Faraday collectors (m/z 44 to 49). Each sample was analyzed for 150 min during which the sample gas and the working reference gas were allowed to flow from volume-matched 10-mL reservoirs into the ion source through a pair of

fused silica capillaries (length: 65 cm, internal diameter: 110 mm). Gas pressures were adjusted to achieve an ion-beam current of 80 nA at m/z = 44, every 20 min, with differences between analyte gas and working gas generally below 0.1 nA. Background currents for each m/z value were measured 12 times (before and after each pressure adjustment) for each analysis. All background measurements within 6 h of any given analysis were used to determine a mass-specific relationship linking background currents to the total amperage measured for m/z = 44 and time for that analysis. Background-corrected ion current (δ_{45} to δ_{49}) values were corrected for oxygen-17 contributions using the IUPAC ¹⁷O correction parameters (Brand et al., 2010) and converted to non-standardized (raw) $\delta^{13}\text{C}$, $\delta^{18}\text{O}$ and Δ_{47} values as described by Daéron et al. (2016). The isotopic compositions ($\delta^{13}\text{C}$ and $\delta^{18}\text{O}$) of the working reference gas CO₂ were computed based on nominal $\delta^{13}\text{C}_{\text{VPDB}}$ and $\delta^{18}\text{O}_{\text{VSMOW}}$ values for carbonate standards ETH-1, ETH-2, ETH-3 reported by Bernasconi et al. (2018), using the value of 1.00813 (Kim et al., 2007a) for ¹⁸O fractionation associated with the 90 °C acid reaction. Raw Δ_{47} values were corrected and normalized to the I-CDES reference frame (Bernasconi et al., 2021) using a pooled regression approach implemented by the D47crunch Python library (Daéron, 2021). Final analytical uncertainties are derived from long-term external reproducibility of samples and standards ($N_f = 338$) and account for standardization errors. The long-term external repeatability of Δ_{47} values for reference materials and unknown samples was 8.6 ppm (1SD, $N_f = 148$) and 7.7 ppm (1SD, $N_f = 190$) respectively. The long-term external repeatability of $\delta^{13}\text{C}_{\text{VPDB}}$ and $\delta^{18}\text{O}_{\text{VSMOW}}$ measurements on carbonate standards was 0.024‰ and 0.042‰, respectively. The full isotopic analysis report for this study can be found in Supplementary data 2.

3.3. Elemental ratio measurements

Concentrations of Mg, Ca and Sr were measured at Institut de Physique du Globe de Paris (IPGP) using an Agilent 7900 quadrupole ICP-MS (Inductively Coupled Plasma Mass Spectrometry). Elemental

concentrations were measured after the following cleaning procedure: specimens were sonicated for 30 s in de-ionized water (resistivity 18 MΩ·cm⁻¹) twice and dried at 50 °C in a drying oven. They were then plunged in a NaOH (0.5 M) + H₂O₂ (15%) solution at 50 °C for 30 min. Cleaned carbonates were then rinsed carefully in de-ionized water, over a 0.2-μm nylon filter mounted on a vacuum filtration unit, and dried overnight at 40 °C in a drying oven under vacuum. Cleaned powdered carbonates were then dissolved in 5% distilled HNO₃ with de-ionized water in an over-pressured and air filtered clean room. A blank sample containing only distilled HNO₃ with de-ionized water prepared in the same condition was also analyzed to track any potential contamination coming from acid or de-ionized water. An internal standard (scandium) was injected just before and after all sample measurements to correct the signal from potential matrix effect and drift during the analytical session. The linear relationship between signal and elemental concentration was established using a set of SPC (Scientific® PlasmaCAL) calibration standards. Uncertainties for each element analyzed were calculated considering the standard deviation on consecutive signal acquisition ($n = 3$) on the same sample and internal standard repeatability (Table 3, Supplementary data 3).

4. Results

4.1. Mineralogy, Mg/ca and Sr/ca ratio

The XRD results on bulk samples from each bryozoan species are summarized in Table 3 and fully reported in Appendix E. Our samples are predominantly composed of Mg-calcite, but certain species are aragonitic (*M. membranacea*) or bimimetic (*P. foliacea*, *C. fistulosa*, *C. pumicosa*, *T. avicularis*) (Fig. 3). We note smaller enrichment in aragonite content in *P. foliacea* (tips) from Roscoff compared to those of Banyuls (i.e., 16 to 23% Aragonite and 77 to 84% Mg-calcite). In addition, the mineralogy of *P. foliacea* also appears to vary with the age of the colony. A decrease in aragonite content in favor of Mg-calcite is observed from the base to the top of this colony.

The Mg/Ca and Sr/Ca ratios of bulk samples range from 19.3 to 118.8 mmol/mol and from 3.2 to 10.5 mmol/mol respectively (Table 3). As expected, these ratios are controlled at first order by skeleton mineralogy. The highest Mg/Ca and lowest Sr/Ca values are obtained for Mg-calcite samples, e.g., *O. ramulosa*. On the contrary, lowest Mg/Ca and highest Sr/Ca values are obtained for predominantly aragonitic

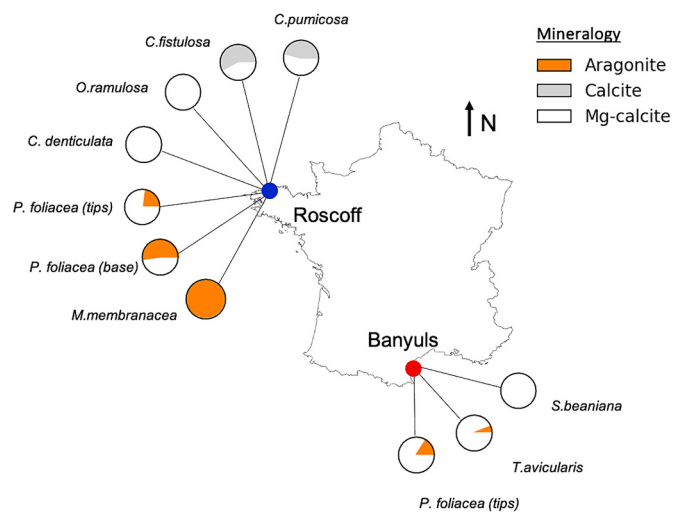


Fig. 3. Mineralogical composition of the different bryozoan samples from Roscoff and Banyuls. Aragonite is represented in orange, calcite in gray and Mg-calcite in white. Pie charts give the mean proportion of aragonite, calcite and Mg-calcite present in the bulk of each species studied (see Table 3).

samples, e.g., *M. membranacea*. Based on Mg/Ca ratio we also calculated the mol % MgCO₃ in each sample. These values are reported in Table 3 and range from 1.60 to 9.08 mol% MgCO₃.

4.2. Stable and clumped-isotope compositions

4.2.1. δ¹⁸O and δ¹³C characterization

Measurements of δ¹⁸O in analyte CO₂ were converted to carbonate δ¹⁸O (VPDB) values (noted δ¹⁸O_c) according to sample's mineralogy and based on "effective" acid fractionation factors for aragonite and calcite (Kim et al., 2007a). We assume that the same fractionation factor applies to Mg-calcite and regular calcite. The δ¹⁸O_c value of bimimetic species was thus calculated taking into account the proportion of aragonite relative to calcite+Mg-calcite:

Table 3

Weight percentage (%) of aragonite, calcite and Mg-calcite and Mg/Ca and Sr/Ca ratios (mmol/mol) in bryozoans bulk samples. For each sample containing more than two mineralogical phases, the error on quantitative calculation of phases ratio is also indicated. The Mg-content in carbonate samples is reported in mol % MgCO₃ based on Mg/Ca ratio.

Sample	Locality	Aragonite (%)	Error (%)	Calcite (%)	Error (%)	Mg-calcite (%)	Mg/Ca (mmol/mol)	2SE	Sr/Ca (mmol/mol)	2SE	mol % MgCO ₃
<i>P. foliacea</i> (tips)	Roscoff	23	1.7	0	0	77	95.62	0.8	5.13	0.04	7.44
<i>P. foliacea</i> (base)	Roscoff	52	1.3	0	0	48	55.89	0.6	7.28	0.08	4.48
<i>C. denticulata</i> (tips)	Roscoff	0	0	0	0	100	84.14	0.7	3.75	0.04	6.60
<i>C. pumicosa</i> (tips)	Roscoff	0	0	46	4.5	54	116.86	0.4	3.51	0.02	8.94
<i>O. ramulosa</i> (tips)	Roscoff	0	0	0	0	100	114.89	0.9	3.22	0.04	8.80
<i>C. fistulosa</i> (tips)	Roscoff	0	0	52	2	48	78.52	0.8	3.52	0.03	6.19
<i>M. membranacea</i> (tips)	Roscoff	100	0	0	0	0	19.30	0.3	10.49	0.10	1.59
<i>S. beaniana</i> (tips)	Banyuls	0	0	0	0	100	110.81	0.3	3.29	0.01	8.52
<i>P. foliacea</i> (tips)	Banyuls	16	3.4	0	0	84	88.89	0.4	4.57	0.02	6.95
<i>T. avicularis</i> (tips)	Banyuls	6	8.4	0	0	94	118.84	0.7	3.65	0.03	9.08

$$\delta^{18}\text{O}_{\text{c}} \text{VPDB} = \frac{\left(\frac{\delta^{18}\text{O}_{\text{CO}_2} \text{VPDB} + 1000}{1.008129} - 1000 \right) \times \% \text{ Calcite or Mg-calcite} + \left(\frac{\delta^{18}\text{O}_{\text{CO}_2} \text{VPDB} + 1000}{1.000041} - 1000 \right) \times \% \text{ Aragonite}}{100}$$

Where $\delta^{18}\text{O}_{\text{CO}_2}$ corresponds to the measured $\delta^{18}\text{O}$ value in the CO_2 gas released during carbonate acid reaction, 1.008129 and 1.000041 correspond, respectively, to the acid fractionation factors for calcite and aragonite (Kim et al., 2007a).

Bryozoan $\delta^{18}\text{O}_{\text{c}}$ values ranged from 0.29‰ to 1.92‰, and $\delta^{13}\text{C}_{\text{VPDB}}$ values ranged from -1.99‰ to 0.7‰ (Table 4). The distributions of $\delta^{13}\text{C}$ and $\delta^{18}\text{O}_{\text{c}}$ values are similar between the two localities, with a pattern of $\delta^{13}\text{C}$ values >2.5‰, and $\delta^{18}\text{O}_{\text{c}}$ values <1‰ (excluding isotopic values for the sample taken from the oldest part of *P. foliacea*, i.e., base).

4.2.2. Clumped-isotope (Δ_{47}) characterization

Clumped-isotope results are summarized in Table 4 and fully reported in Supplementary data 2. Our measured Δ_{47} values range from 0.652‰ to 0.630‰. We found up to 0.0223‰ difference in clumped-isotope values between species coming from the same locality (i.e., Roscoff) and thus grown under the same environmental conditions (i.e., temperature). This range of Δ_{47} values is >95% confidence level (CL) on measurements (~0.006 to ~0.008). By contrast, species from Banyuls yield indistinguishable Δ_{47} values between each other with respect to 95% CL. More surprisingly, *P. foliacea* tips from Banyuls give Δ_{47} values significantly higher (0.0139‰) than those obtained from *P. foliacea* tips coming from Roscoff. This is contrary to the decrease Δ_{47} value expected with increasing seawater temperature at Banyuls (Fig. 4). We find that Δ_{47} values of *P. foliacea* tips, *C. pumicosa*, *O. ramulosa* and *C. fistulosa* from Roscoff are consistent, within uncertainties, with the OGSL23 calibration recently compiled by Daéron and Vermeesch (2024) (Fig. 4). The 3 remaining species (*M. membranacea*, *P. foliacea* base and *C. denticulata*) yield Δ_{47} values 12.3 to 22.9 ppm greater than expected. The maximum offset from the OGSL23 equilibrium line is observed for the aragonite species *M. membranacea* (Fig. 4). By contrast, all Banyuls samples yield greater than expected Δ_{47} values.

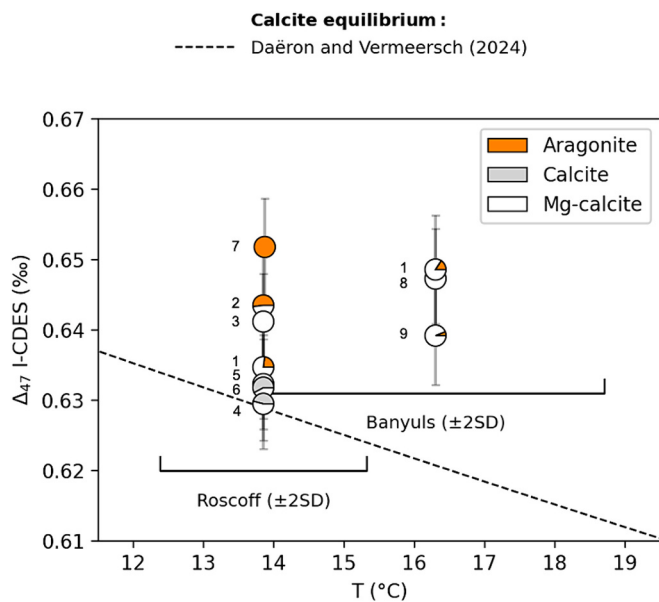


Fig. 4. Measured Δ_{47} versus local seawater temperature measured in-situ during bryozoan growth. The average temperature during bryozoan growth period is indicated for each site based on in-situ temperature record. Horizontal brackets correspond to the 2SD around this calculated average temperature during bryozoan growth period reflecting seasonal temperature variability typical of costal environments. Samples mineralogical content are also indicated (aragonite in orange, calcite in gray and Mg-calcite in white). The OGSL23 Δ_{47} calibration line (Daéron and Vermeesch, 2024), considered as the equilibrium value, is shown as a black dashed line. Numbering of pie charts refers to the different bryozoan species; 1- *P. foliacea* (tips), 2- *P. foliacea* (base), 3- *C. denticulata*, 4- *C. pumicosa*, 5- *O. ramulosa*, 6- *C. fistulosa*, 7- *M. membranacea*, 8- *S. beaniana*, 9- *T. avicularis*.

Table 4

Number of replicates (n) and mean oxygen and carbon stable and clumped-isotope compositions of bryozoan samples. All isotopic compositions are reported in per mill. The $\delta^{18}\text{O}_{\text{CO}_2}$ (VSMOW) was converted to $\delta^{18}\text{O}_{\text{c}}$ (VPDB) according to samples mineralogical content and the acid fractionation factors (see eq. 1). The $^{18}\alpha_{\text{w-c}}$ values were calculated from $\delta^{18}\text{O}_{\text{c}}$ with respect to the $\delta^{18}\text{O}_{\text{sw}}$ values estimated from salinity records at both sites (Table 1). Clumped-isotope are reported in the I-CDES reference scale.

Sample	Locality	n	$\delta^{13}\text{C}_{\text{c}}$ VPDB (‰)	2SE (‰)	$\delta^{18}\text{O}_{\text{CO}_2}$ VSMOW (‰)	$\delta^{18}\text{O}_{\text{c}}$ VPDB (‰)	2SE (‰)	$^{18}\alpha_{\text{w-c}}$ (‰)	2SE (‰)	Δ_{47} I-CDES (‰)	95% CL (‰)
<i>P. foliacea</i> (tips)	Roscoff	7	0.38	0.02	39.93	0.51	0.04	1.0310	0.06	0.6347	0.0073
<i>P. foliacea</i> (base)*	Roscoff	15	0.63	0.02	41.51	1.91	0.03	1.0324	0.05	0.6435	0.0086
<i>C. denticulata</i> (tips)	Roscoff	7	-0.3	0.01	39.77	0.45	0.03	1.0309	0.05	0.6412	0.0068
<i>C. pumicosa</i> (tips)	Roscoff	9	-1.19	0.02	39.60	0.29	0.03	1.0308	0.05	0.6295	0.0064
<i>O. ramulosa</i> (tips)	Roscoff	9	-0.81	0.02	39.97	0.64	0.03	1.0311	0.05	0.6323	0.0064
<i>C. fistulosa</i> (tips)*	Roscoff	12	0.70	0.02	40.13	0.79	0.03	1.0313	0.05	0.6318	0.0075
<i>M. membranacea</i> (tips)	Roscoff	7	-1.70	0.01	40.09	0.35	0.03	1.0308	0.05	0.6518	0.0069
<i>S. beaniana</i> (tips)	Banyuls	7	0.43	0.02	41.20	1.83	0.04	1.0314	0.21	0.6473	0.0071
<i>P. foliacea</i> (tips)	Banyuls	6	0.02	0.02	41.37	1.92	0.04	1.0315	0.21	0.6486	0.0077
<i>T. avicularis</i> (tips)	Banyuls	7	-1.99	0.02	40.46	1.09	0.05	1.0307	0.21	0.6392	0.007

*Average $\delta^{18}\text{O}$, $\delta^{13}\text{C}$ and Δ_{47} values obtained during the cleaning test phase (protocol 2 and equivalent 2b) and samples prepared for interspecies comparison.

5. Discussion

5.1. Characterization of oxygen and carbon isotope fractionation between bryozoans and seawater

5.1.1. Bryozoan $\delta^{18}\text{O}$ and $\delta^{13}\text{C}$ positive correlation

Oxygen and carbon isotopes between species from the same locality are much more scattered than might be expected a priori in organisms grown under the same environmental conditions (Table 4). At both sites, $\delta^{13}\text{C}$ and $\delta^{18}\text{O}$ values tend to be weakly correlated, with similar positive slopes of 0.34 vs 0.38 at Banyuls and Roscoff, respectively, consistent with previous bryozoan studies (Crowley and Taylor, 2000; Smith and Key, 2004; Bader and Schäfer, 2005) (Fig. 5a). The ^{18}O fractionation between calcite and water ($^{18}\alpha_{\text{w-c}}$) and ^{13}C fractionation between calcite and DIC ($^{13}\alpha_{\text{DIC-c}}$) are potentially affected by Mg substitution within the crystal lattice (Tarutani et al., 1969; Jiménez-Lopez et al., 2004, 2006; Mavromatis et al., 2012). Based on experimental precipitation of Mg-enriched calcite, Tarutani et al. (1969) proposed that ^{18}O fractionation factor increases by 0.06‰ per mol % MgCO_3 . This number was revisited by Jimenez-Lopez et al. (2004) and Mavromatis et al. (2012) based on new experiments respectively yielding factors of +0.17‰ and +0.18‰ per mol % MgCO_3 . Concerning ^{13}C fractionation, Jimenez-Lopez et al. (2006) reported 0.024‰ enrichment per mol % MgCO_3 . Because our samples contain a substantial amount of MgCO_3 (Table 3) we may look for potential Mg effect on bryozoan ^{13}C and ^{18}O records by testing whether correcting isotopic value from Mg substitution would modify $^{13}\alpha_{\text{DIC-c}}$ and $^{18}\alpha_{\text{w-c}}$ distribution (range and slope). We tested this assumption applying Tarutani et al. (1969) and Mavromatis et al. (2012) correction factor to our $^{18}\alpha_{\text{w-c}}$ values and Jimenez-Lopez et al. (2006) correction factor to our $^{13}\alpha_{\text{DIC-c}}$ values. At face value, applying Mg correction slightly modifies the $1000\ln^{13}\alpha_{\text{DIC-c}}$ and $1000\ln^{18}\alpha_{\text{w-c}}$ by decreasing them (Fig. 5b). However, doing so does not substantially

affect the offset between species and the correlation between $1000\ln^{13}\alpha_{\text{DIC-c}}$ and $1000\ln^{18}\alpha_{\text{w-c}}$. Thus, Mg substitution alone does not explain the spreading of $\delta^{13}\text{C}$ and $\delta^{18}\text{O}$ values of bryozoans. Some other biocarbonates exhibit also a positive correlation between $\delta^{13}\text{C}$ and $\delta^{18}\text{O}$, such as corals (e.g., McConaughey, 1989a; Smith et al., 2000; Adkins et al., 2003; Rollion-Bard et al., 2003a; Blamart et al., 2005), brachiopods (e.g., Auclair et al., 2003; Parkinson et al., 2005; Rollion-Bard et al., 2016; Bajnai et al., 2018), or cephalopods (Chung et al., 2021). It has been proposed that these correlations could be related to kinetic isotope effects (KIEs) within the $\text{DIC}-\text{CO}_2-\text{H}_2\text{O}$ system before precipitation (McConaughey, 1989b), to pH-dependent effects occurring at the fluid – CaCO_3 interface (Adkins et al., 2003), or to a combination of both (Rollion-Bard et al., 2003b, 2010). This could also be the case in bryozoans.

5.1.2. Does $\delta^{18}\text{O}$ thermometry apply to bryozoan CaCO_3 ?

Partitioning of oxygen isotopes between calcium carbonate, water and DIC at low temperatures (0–50 °C) forms the basis of the oldest and most widely-used stable isotope paleothermometer (Urey, 1947; Epstein et al., 1953). Barring large isotopic disequilibrium, the $\delta^{18}\text{O}$ of carbonates should reflect both the temperature and the $\delta^{18}\text{O}$ of the fluid from which they formed (Urey, 1947), making carbonate $\delta^{18}\text{O}$ records the cornerstone of paleoclimate reconstructions since >70 years. Urey's prediction, however, came with the caveat that "whether animals lay down carbonates in equilibrium with water" remained a working hypothesis. Obviously, chemical/isotopic equilibrium *stricto sensu* implies that chemical/isotopic fluxes are perfectly balanced, precluding net growth of the mineral. One may nevertheless propose that, in slightly saturated systems where the ratio of crystallization to dissolution tends toward one, the effective ^{18}O fractionation between water and carbonate may be indistinguishable from its equilibrium limit (e.g., Gabitov et al., 2012; Watkins et al., 2014; Devriendt et al., 2017), so that ^{18}O

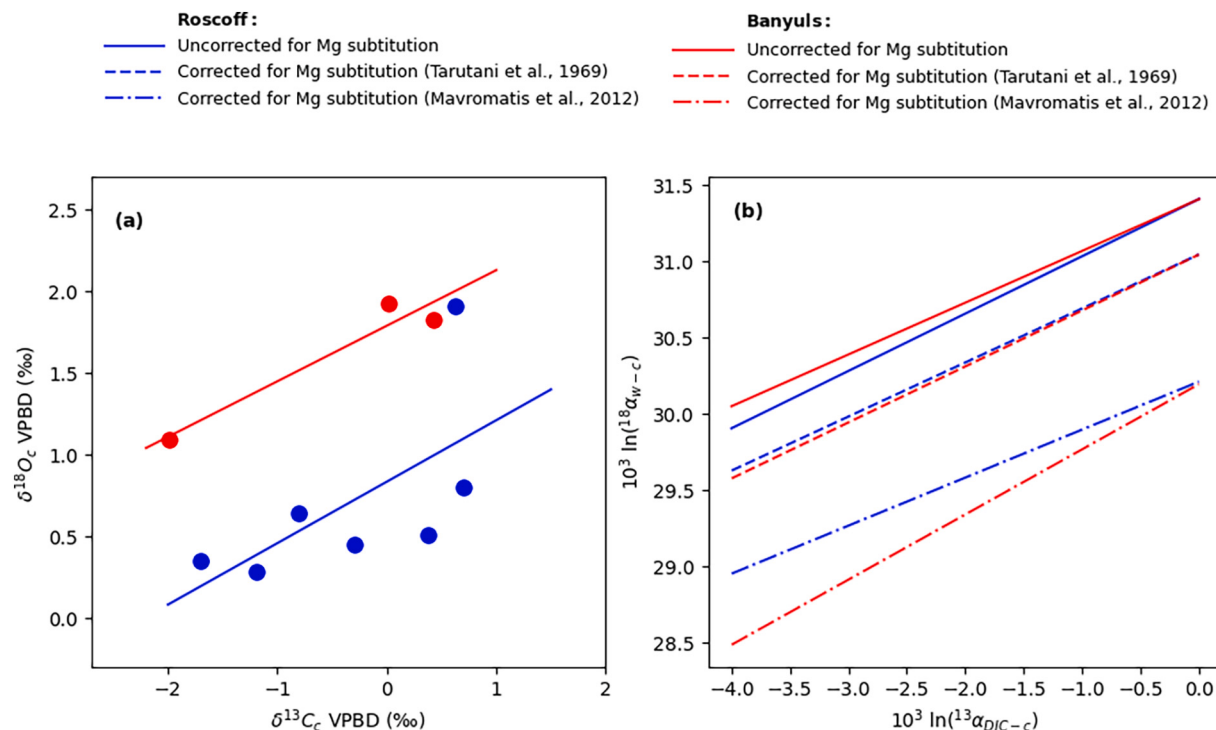


Fig. 5. (a) Distribution of bryozoan $\delta^{13}\text{C}$ and $\delta^{18}\text{O}$ values excluding entirely aragonitic sample (*M. membranacea*) and (b) calculated $1000\ln^{13}\alpha_{\text{DIC-c}}$ and $1000\ln^{18}\alpha_{\text{w-c}}$ as a function of sampling localities (Banyuls: red, Roscoff: blue) and with respect to environmental record. (a) Solid lines describe the general trend between $\delta^{13}\text{C}$ and $\delta^{18}\text{O}$ values. (b) Corresponds to a comparison between $1000\ln^{13}\alpha_{\text{DIC-c}}$ and $1000\ln^{18}\alpha_{\text{w-c}}$ before (solid line) and after correction for Mg substitution effect on $1000\ln^{13}\alpha_{\text{DIC-c}}$ and $1000\ln^{18}\alpha_{\text{w-c}}$ with respect for enrichment factor defined by Jiménez-Lopez et al. (2006) for $1000\ln^{13}\alpha_{\text{DIC-c}}$ and Tarutani et al. (1969) (dashed lines) or Mavromatis et al. (2012) (semi-dotted line) for $1000\ln^{18}\alpha_{\text{w-c}}$. (For interpretation of the references to colour in this figure legend, the reader is referred to the web version of this article.)

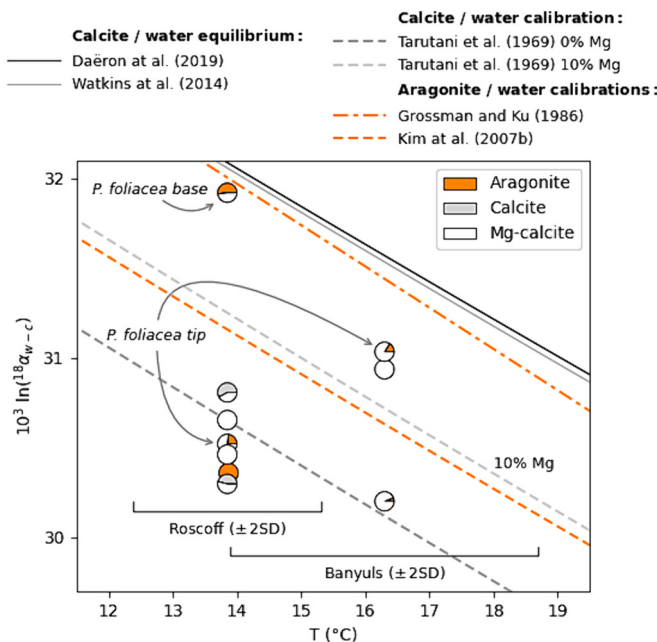


Fig. 6. ^{18}O fractionation between water and bryozoan carbonate ($1000\ln^{18}\alpha_{w-c}$) as a function of growth temperature measured in-situ. The mineralogical proportions are represented in each circle with orange for aragonite, gray for calcite and white for Mg-calcite. The $^{18}\alpha_{w-c}$ /temperature relationships documented in the literature are also reported for aragonite (orange - Grossman and Ku, 1986; Kim et al., 2007b), calcite (black/gray - Tarutani et al., 1969; Watkins et al., 2014; Daëron et al., 2019) and Mg-calcite containing 10 mol% of MgCO_3 (light gray - Tarutani et al., 1969).

fractionation at equilibrium may be constrained by studying natural calcites formed at extremely slow growth rates, not achievable in laboratory calibration studies (Coplen, 2007; Levitt et al., 2018; Daëron et al., 2019). However, a growing body of evidence implies that such ^{18}O quasi-equilibrium is very rarely achieved at Earth surface conditions, because natural carbonates (particularly biogenic ones) most often precipitate very fast from supersaturated solutions. Nevertheless, in various laboratory experiments (e.g., Tarutani et al., 1969; Kim and O'Neil, 1997; Kim et al., 2007b), as well as in various biocarbonates (e.g., Grossman and Ku, 1986; Anderson and Arthur, 1983; Daëron and Gray, 2023), oxygen isotope fractionation between water and CaCO_3 ($^{18}\alpha_{w-c}$) appears to vary primarily with calcification temperature in a predictable way, with $^{18}\alpha_{w-c}$ /temperature slopes indistinguishable from that of $^{18}\alpha$ between carbonate ions and water ($\sim 0.21\text{‰}$ per degree at $\sim 25\text{ }^\circ\text{C}$). Early studies of bryozoan oxygen isotopes thus assumed that $^{18}\alpha_{w-c}$ of bryozoans would follow or approximate relationships documented in experimental precipitates and biocarbonates (Rao and Nelson, 1992; Bone and James, 1997; Key et al., 2013). On the other hand, later studies have raised the possibility of bryozoan “vital effects” (Crowley and Taylor, 2000; Smith et al., 2004; Nehyba et al., 2008) potentially making $^{18}\alpha_{w-c}$ sensitive to parameters other than temperature. We may look for such vital effects in our data set by checking whether different bryozoan species from the same locality display similar ^{18}O values, with perhaps small differences arising from mineralogy, and whether the temperature sensitivity documented by *P. foliacea* between Roscoff and Banyuls differs from that expected for “classical” ^{18}O thermometry.

As seen in Fig. 6, $1000\ln^{18}\alpha_{w-c}$ values for colony tips within each site are only moderately scattered ($\pm 0.25\text{‰}$). This scatter is not greater than that expected based on the temperature variability recorded in-situ during the probable bryozoan growth period (April to October). However, we note that the $1000\ln^{18}\alpha_{w-c}$ value of the fully aragonitic bryozoan (*M. membranacea*) is lower than the $1000\ln^{18}\alpha_{w-c}$ values of most

calcite-enriched samples (Fig. 6), which is not consistent with the expected 0.6 to 0.75‰ enrichment in ^{18}O in aragonite relative to calcite (Tarutani et al., 1969; Zhou and Zheng, 2005; Kim et al., 2007b). Furthermore, $1000\ln^{18}\alpha_{w-c}$ for *P. foliacea* at Banyuls is about 0.5% greater than for *P. foliacea* at Roscoff. This is at odds with the fact that Banyuls seawater is on average $2.5\text{ }^\circ\text{C}$ warmer than at Roscoff, which should decrease $1000\ln^{18}\alpha_{w-c}$ by 0.5%. Although we did not directly measure seawater ^{18}O , our $^{18}\text{O}_{\text{sw}}$ estimates, derived from local salinity, are consistent with regional values (LeGrande and Schmidt, 2006), with Mediterranean Sea $^{18}\text{O}_{\text{sw}}$ about 1% greater than North Atlantic ones. It is thus likely that $^{18}\alpha_{w-c}$ at one or both sites is sensitive to additional biological and/or environmental factors beyond temperature and seawater ^{18}O .

Finally, we find that ^{18}O values at the base of *P. foliacea* (i.e., the oldest part of the skeleton) are heavily enriched ($+1.4\text{‰}$) relative to the tips of the same colony (Table 4, Fig. 6). *Pentapora foliacea* may grow over several years (Pätzold et al., 1987) or decades (Cocito et al., 1998) with typical growth rates ranging from 1 to 2 cm/yr . This implies that the age difference between our tip and base samples does not exceed 15 years. Average local seawater temperature has not risen by $>1.5\text{ }^\circ\text{C}$ over the past 15 years, as attested by the weekly temperature record at Astan station (www.somlit.fr). The isotopic difference between *P. foliacea* base and tips is thus unlikely to reflect environmental changes exclusively.

On the other hand, enriched ^{18}O values at the base of *P. foliacea* suggest that the oldest part of *P. foliacea* would have formed during colder period ($\pm 8.8\text{ }^\circ\text{C}$). According to the seawater temperature readings at the Astan station, coldest temperatures are reached in February and range from 8.79 to $10.5\text{ }^\circ\text{C}$ (www.somlit.fr). We cannot exclude that bryozoan growing period evolves during the whole colony lifespan. However, in 1998, Cocito et al. noted the absence of ovicells (i.e., dilatation of the zooecium wall in which ova developed) in *P. foliacea* from October to February by monitoring growth and mortality of Mediterranean *P. foliacea* colonies over an entire year. Over the same period, they also reported zero and even negative colony’s growth. Thus, it is also unlikely that the base of *P. foliacea* had formed in February. It is also interesting to note that $^{18}\alpha_{w-c}$ values of the colony base lie pretty close ($<0.2\text{‰}$ away) to those predicted by Daëron et al. (2019) and Watkins et al. (2014) for calcite/water equilibrium, while those from the tips lie on the calibration from Tarutani et al. (1969) established from laboratory precipitated calcite (Fig. 6). The calcite/water equilibrium was established based on the oxygen isotopic composition of natural calcites from cave (Coplen, 2007; Daëron et al., 2019). Since they were formed extremely slowly under stable environmental conditions, the composition of these two natural samples are considered to record equilibrium values of $^{18}\alpha_{w-c}$. Bryozoan growth rate typically ranges from 1.10^{-7} to $4.10^{-7}\text{ mol.m}^{-2}.\text{s}^{-1}$ (Cocito and Ferdeghini, 2001), which is about 3 orders of magnitude faster than the natural slow-growing calcites used to constrain equilibrium ^{18}O fractionation ($1-8.10^{-10}\text{ mol.m}^{-2}.\text{s}^{-1}$, Coplen, 2007; Daëron et al., 2019). Cocito et al. (1998) have shown that *P. foliacea* grows even faster in its early stages than during the rest of its life. Several evidences for such “ontogenetic effects” (also known as the “astrogenetic effect” in the case of colonial organisms) on $^{18}\alpha_{w-c}$ values exists in the literature (e. g., Huyghe et al., 2020; Davies et al., 2021). Contrary to observed increase in $^{18}\alpha_{w-c}$ values of *P. foliacea* early stage, astrogenetic effects on $^{18}\alpha_{w-c}$ values are characterized by ^{18}O depletion which is supposed to be controlled by CO_2 absorption kinetics during rapid CaCO_3 accretion (Spero and Lea, 1996; Goodwin et al., 2003; Huyghe et al., 2020; Davies et al., 2021). In this way, neither astrogenetic effects nor environmental changes explain intra-colonial isotopic discrepancies. One last potential explanation would be the alteration from the oldest part of the *P. foliacea* skeleton. Recently, Batson et al. (2020) investigated bryozoan skeleton resorption capacity. Their review revealed the incredible plasticity of the colony’s skeleton and showed that after initial formation colony structures can change in two ways: I) the secretion or removal of CaCO_3 mineral; II) skeletal resorption that renovate or remove an already-functioning skeletal

element in the secondary zone of the colony (the oldest part). The extent of this alteration process can go from the microscopic to the colony-wide scale and occurs in the next one to ten years after initial skeleton precipitation (Batson et al., 2020). Isotopic and mineralogical changes observed between the base and the top of the *P. foliacea* colony could result from resorption transforming the calcite to aragonite in the oldest parts of the colony. In this way, the elevated $\delta^{18}\text{O}_{\text{w-c}}$ value from the base of the *P. foliacea* could be related to KIEs arising from physiologically controlled dissolution and reprecipitation of the skeleton during colony reshaping (Watkins et al., 2013, 2014; Devriendt et al., 2017). At this point, resorption effects on isotopic fractionation seem to be the most likely hypothesis that justifies isotopic evolution along the bryozoan skeleton. Further information on the development of the different calcium carbonate polymorphs within the bryozoan skeleton and their spatial and temporal evolution at the colony scale would be particularly helpful to settle this issue.

5.1.3. Is bryozoan $\delta^{13}\text{C}$ composition influenced by metabolic sources?

The $\delta^{13}\text{C}$ recorded in marine biocalcifiers is influenced by two main factors: the $\delta^{13}\text{C}$ of seawater DIC and the metabolic $\delta^{13}\text{C}$, which refers to the $\delta^{13}\text{C}$ derived from respired CO_2 product (mitochondrial respiration). Bryozoan $\delta^{13}\text{C}$ values are broadly scattered at Roscoff and Banyuls ($\pm 1.2\text{\textperthousand}$) and almost cover the same range of values. While the average $\delta^{13}\text{C}$ of bryozoans does not differ markedly between the two sites, we note that *P. foliacea* tips samples show a slight decrease in their $\delta^{13}\text{C}$ values between Roscoff and Banyuls ($\sim 0.36\text{\textperthousand}$). This is in line with the slightly lower $\delta^{13}\text{C}$ values of the DIC at Banyuls compared to Roscoff (Table 1).

The $\delta^{13}\text{C}$ fractionation factor between HCO_3^- and CaCO_3 was given by Romanek et al. (1992), who measured that calcite and aragonite should respectively be enriched by 1\textperthousand and $2.7\text{\textperthousand}$ in ^{13}C compared to bicarbonate ions in solution. Regardless of the sampling site, we can affirm, on the basis of seawater pH record, that DIC mostly derived from bicarbonate ions. Based on this assumption, we calculated predicted $\delta^{13}\text{C}$ values of bryozoan if they were exclusively derived from seawater DIC (Supplementary data 1, Table. B.2). As already observed in bryozoan by Crowley and Taylor (2000), comparison between measured $\delta^{13}\text{C}$ and the predicted value by Romanek et al. (1992) yields large discrepancies (i.e., up to $-5.90 \pm 0.51\text{\textperthousand}$). Such depletion in $\delta^{13}\text{C}$ could suggest that at least one carbon source other than seawater DIC contributes to bryozoan skeleton carbon isotopic composition. Apart from DIC, metabolic CO_2 was already shown to be a substantial source of carbon, as for example in corals where it reaches up to 75% contribution (Furla et al., 2000).

As a general view, CO_2 derived from metabolic processes is largely depleted in ^{13}C (up to $-25\text{\textperthousand}$, e.g., Blamart et al., 2005) and ^{18}O . Applying simple mass balance calculation and considering a $\delta^{13}\text{C}$ of metabolic CO_2 of $-25\text{\textperthousand}$, we estimated that between 10% to 30% of the respiratory CO_2 could contribute to carbon uptake within bryozoan CaCO_3 . On the other hand, bryozoan $\delta^{13}\text{C}$ record could also be affected by kinetic isotope fractionation within the DIC- CO_2 - H_2O system before precipitation as attested by $\delta^{13}\text{C}$ - $\delta^{18}\text{O}$ covariation (Fig. 5a). As a matter of fact, CO_2 (de)hydration and (de)hydroxylation reactions taking place within the DIC- CO_2 - H_2O system are characterized by slow exchange rates. In the context of rapid CaCO_3 precipitation, where all reactions are pushed forward to convert CO_2 to HCO_3^- (as it is the case during biocalcification), isotopic equilibrium between DIC, water and CO_2 may not be maintained, as (de)hydration and (de)hydroxylation reactions occur slower than precipitation (e.g., McConaughey, 1989b; Chen et al., 2018) resulting in a synchronous depletion of heavy isotopes (^{18}O and ^{13}C) in biocarbonate (e.g., McConaughey, 1989b; Chen et al., 2018; Guo, 2020; Watkins and Devriendt, 2022). Already proposed as a potential explanation for positive $\delta^{13}\text{C}$ - $\delta^{18}\text{O}$ correlation observed in various types of biocarbonate, the influence of kinetic effects on bryozoan $\delta^{13}\text{C}$ and $\delta^{18}\text{O}$ records has remained unclear until now. The good agreement between our data with previous anomalous $\delta^{13}\text{C}$ - $\delta^{18}\text{O}$ records in other types of biocarbonates (i.e., brachiopods, cold-water

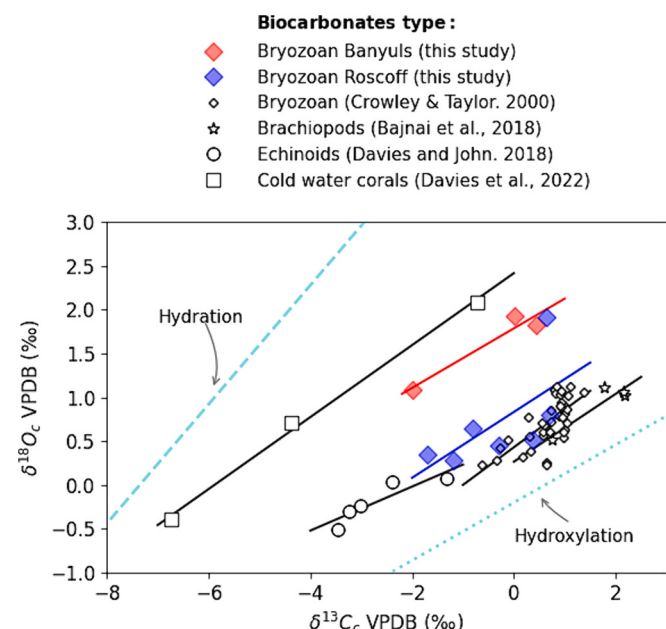


Fig. 7. Comparison of bryozoan $\delta^{13}\text{C}$ - $\delta^{18}\text{O}$ correlation slope (in blue: Roscoff sample, in red: Banyuls sample) with other biocarbonates from the literature known to be affected by KIEs; open circle: echinoids *Strongylocentrotus droebachiensis* (Davies and John, 2019), open star: temperate brachiopods (Bajnai et al., 2018), open square: cold water corals (Davies et al., 2022). For comparison purpose we also reported $\delta^{13}\text{C}$ and $\delta^{18}\text{O}$ values of bryozoan samples from Otago shell (black diamonds) previously published by Crowley and Taylor (2000). For data from the literature shown here, we only reported isotopic composition of biocarbonates grown in the same environmental conditions so that $\delta^{13}\text{C}$ - $\delta^{18}\text{O}$ correlation does not result from change in temperature, $\delta^{18}\text{O}_{\text{w}}$ nor $\delta^{13}\text{C}_{\text{DIC}}$. Are also shown the expected correlation slopes between $\delta^{13}\text{C}$ and $\delta^{18}\text{O}$ resulting from KIEs during CO_2 hydration (cyan dashed line) and hydroxylation (cyan dotted line) by Guo (2008). (For interpretation of the references to colour in this figure legend, the reader is referred to the web version of this article.)

corals, echinoids) where the influence of KIEs was confirmed, supports that bryozoan isotopic composition is affected by small but existent disequilibrium potentially related to KIEs during CO_2 (de)hydroxylation (Fig. 7).

5.2. Bryozoan growth temperature derived from clumped-isotope thermometry

Because clumped-isotope thermometry does not require any a priori knowledge on the isotopic composition of the calcification fluid (Schauble et al., 2006), one could expect that bryozoans Δ_{47} signatures strictly reflect environmental temperature recorded between April and October. Although establishing a universally applicable Δ_{47} calibration has long remained challenging, at least in part due to subtle inter-laboratory differences (Petersen et al., 2019), the recent definition of a new metrological scale for Δ_{47} appears to have solved these issues (Bernasconi et al., 2021), effectively reconciling previously discrepant calibrations studies (Anderson et al., 2021; Daëron and Vermeesch, 2024). Here we use the OGSL23 composite calibration based on ~ 100 (mostly calcitic) samples, with formation temperatures ranging from 0 to $1100\text{ }^{\circ}\text{C}$ (Daëron and Vermeesch, 2024). Comparing growth temperatures estimated from in situ observations (T_{obs}) to those derived from clumped-isotope (T_{47}), we find that most Roscoff samples have T_{47} values generally consistent with the lower range of T_{obs} , except for *M. membranacea* for which $T_{47} < T_{\text{obs}}$ (Fig. 8 top panel). By contrast, all samples from Banyuls have T_{47} values about 5 to $8\text{ }^{\circ}\text{C}$ colder than the local mean annual temperature (Fig. 8 top panel). In order to better

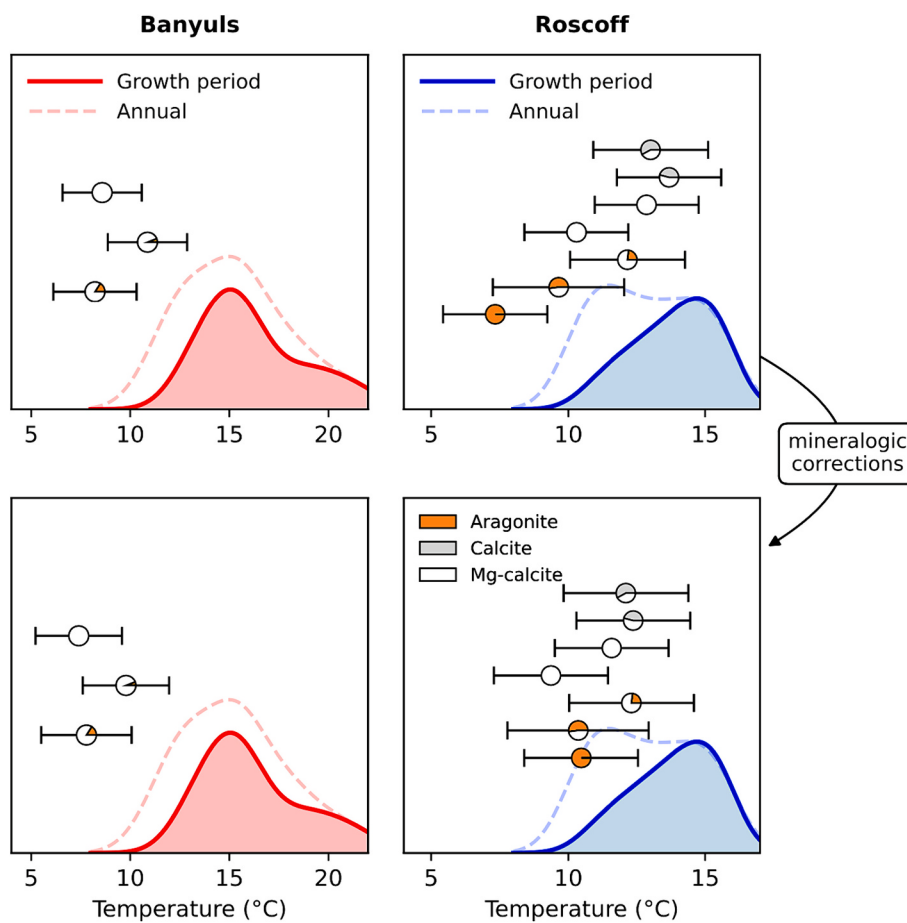


Fig. 8. Comparison, for bryozoan samples from Banyuls (left-red) and Roscoff (right-blue), of local seawater temperature (bottom curves) based on weekly in situ record (T_{obs}) and apparent calcification temperatures derived from Δ_{47} (T_{47} derived from OGGS23). Colored bell-shaped curves represent the temperature distributions over the most likely growth period of bryozoans. The distribution of temperature all year round is also shown (Colored dashed curves). Mineralogical contents for each sample are indicated (aragonite: orange, calcite: gray, Mg-calcite: white). The position of each pie chart relative to x-axis is determined by T_{47} derived from OGGS23 only (top panel) and from OGGS23 taking into account of the mineralogical effect on Δ_{47} predicted by Hill et al. (2020) (bottom panel). For complementary information about mineralogical effect on Δ_{47} see text (section 5.3.1). (For interpretation of the references to colour in this figure legend, the reader is referred to the web version of this article.)

constrain the sources for positive offset in Δ_{47} from bryozoan, we may look for potential mineralogical effects on T_{47} by checking whether Δ_{47} covariates with bryozoan mineralogical properties, and Δ_{47} sensitivity to environmental parameters other than temperature documented by *P. foliacea* between Roscoff and Banyuls.

5.3. On the positive offset in bryozoan Δ_{47}

5.3.1. Mineralogical effects on Δ_{47} equilibrium

At Roscoff, aragonitic samples yield higher Δ_{47} values than others. This is qualitatively consistent with the theoretical predictions of Hill et al. (2020), who predicted that equilibrium Δ_{47} values should be 12 ppm greater for aragonite than for calcite at ambient temperatures. Conversely, the substitution of Ca for Mg in the crystal lattice tends to lower equilibrium Δ_{47} values (by 5 ppm for a 10% enrichment in Mg). Previous T_{47} calibrations almost exclusively include calcite or low magnesium calcite samples (Anderson et al., 2021; Fiebig et al., 2021; Daéron and Vermeesch, 2024) and have been shown to be consistent with theoretically predicted calcite equilibrium Δ_{47} values. De Winter et al. (2022) recently investigated the temperature dependence of Δ_{47} in aragonite bivalve shells (*A. islandica*), obtaining Δ_{47} values greater than predicted by the largely inorganic calibration of Anderson et al. (2021) but consistent on average with an alternative Δ_{47} calibration based on planktic foraminifera (Meinicke et al., 2020). Proposing that the

Anderson et al. calibration underestimates T_{47} by 2.7 °C in carbonates formed at low temperatures (0–18 °C), they argued against the need for mineralogy-specific Δ_{47} calibrations. Since then, Daéron and Gray (2023) re-assessed the calcification temperatures in several foraminifer calibration data sets, concluding that the Meinicke et al. (2020) calibration over-estimates foraminifer calcification temperatures by 2–3 °C at low temperatures, and that using updated species-specific oxygen-18 calibrations reconciles foraminifer Δ_{47} calibrations with inorganic calibrations believed to constrain equilibrium Δ_{47} values (Anderson et al., 2021; Fiebig et al., 2021, both of which contribute heavily to the combined OGGS23 calibration used in this study). Finally, we now have additional “cold” constraints from *A. pecten* shells that formed at –1.8 °C (Huyghe et al., 2022), which appear fully consistent with Anderson et al. (2021). In light of the above, we propose that De Winter et al.’s (2022) conclusion may be re-assessed. We note, in particular, that the average Δ_{47} residuals between their four *A. islandica* samples and the OGGS23-predicted equilibrium Δ_{47} values is $+10 \pm 4$ ppm (95% CL, cf. fig. B.7 of Supplementary data 1), consistent with the theoretical offset between aragonite and calcite (Hill et al., 2020).

Fig. 8 shows how correcting previous calibrations for mineralogical effects would offset our T_{47} values. At Roscoff, these corrections reconcile the T_{47} values obtained for each bryozoan species and tend to suppress, at least partially, the apparent offsets between T_{47} and T_{obs} . While the average T_{47} remains 2–3 °C colder than the temporal average

of environmental temperatures, it is debatable whether this reflects systematic isotopic disequilibrium or reduced growth in the summer.

The same cannot be said, however, of the Banyuls samples, for which Δ_{47} values remain substantially colder than the environmental temperature minimum even after mineralogical correction. Banyuls samples are more homogenous both in mineralogy and in uncorrected Δ_{47} values which in itself is not contradictory with potential mineralogical effects on Δ_{47} . The fact that the Banyuls samples yield much greater Δ_{47} than expected thus point to a source of disequilibrium other than mineralogy.

5.3.2. Potential effect of environmental parameter other than temperature on Δ_{47} equilibrium

Positive Δ_{47} offsets from equilibrium values have been widely documented in the literature and are often thought to be related to kinetic isotope effects associated with rapid CO_2 absorption (Guo, 2020). Such offsets have been reported in corals (Thiagarajan et al., 2011; Saenger et al., 2012; Spooner et al., 2016; Davies et al., 2022), brachiopods (Bajnai et al., 2018; Letulle et al., 2023; Davies et al., 2023), cephalopods (Davies et al., 2021), and echinoids (Davies and John, 2019). The same explanation could also apply to bryozoans, but we still need to account for the fact that only bryozoans from one site (Banyuls) are clearly offset from equilibrium regarding Δ_{47} values. A natural hypothesis is that this is due to environmental differences between the two sites, with the most obvious chemical differences being pH and salinity (Table 1). Although previous studies have so far reported that Δ_{47} thermometry appears insensitive to pH or salinity in other organisms such as foraminifera (e.g., Tripati et al., 2010; Peral et al., 2018), these two factors are known to directly or indirectly influence isotopic fractionations in the $\text{H}_2\text{O}-\text{DIC}-\text{CaCO}_3$ system.

The distribution of DIC species between $\text{CO}_2(\text{aq})$, HCO_3^- and CO_3^{2-} is primarily controlled by pH. Banyuls seawater has an average pH value about 0.2 units higher than Roscoff seawater, favoring CO_3^{2-} over HCO_3^- . From theoretical calculations, Hill et al. (2014) reported that $\Delta_{63}(\text{H}_2\text{CO}_3) > \Delta_{63}(\text{HCO}_3^-) > \Delta_{63}(\text{CO}_3^{2-})$ with CO_3^{2-} depleted about 0.033% in Δ_{63} compared to HCO_3^- (Δ_{63} being the DIC equivalent of Δ_{47} in CO_2 , primarily tracing the excess of ^{13}C — ^{18}O bonds in the (bi)carbonate ions). Assuming that bryozoan Δ_{47} signatures are directly inherited from the average Δ_{63} values of DIC (such as would be the case if the DIC was rapidly and quasi-quantitatively precipitated at the calcifying sites), an increase in pH should decrease Δ_{47} which is the reverse of our observation. On the other hand, an increase in pH should simultaneously decrease the rate of isotope exchange between DIC and water and increase the relative contribution of CO_2 hydroxylation vs hydration (e.g., Johnson, 1982) potentially promoting increase of Δ_{47} of the DIC pool (Watkins and Hunt, 2015; Uchikawa et al., 2021; Guo, 2020). Nevertheless, seawater pH may not be directly relevant in this case, particularly if bryozoans exert a strong control on pH at the calcifying site, as do many other biocalcifiers (e.g., Blamart et al., 2007; Rollion-Bard et al., 2003b, 2010; Allison and Finch, 2010; Rollion-Bard and Erez, 2010; McCulloch et al., 2012). A potential way to test this hypothesis would be to measure the boron isotopes ($\delta^{11}\text{B}$) composition of bryozoan in order constrain calcification pH (e.g., Hemming and Hanson, 1992). The absence of such data prevents us from going any further on this subject, for time being.

Contrary to pH, calcifying fluid salinity is more likely to closely reflect seawater salinity because marine calcifiers are generally unable to strongly regulate Na^+ and Cl^- concentrations (e.g., Erez, 2003; Gray et al., 2023). Although increased salinity at a given pH will slightly reduce pK_2 (increasing the ratio of CO_3^{2-} over HCO_3^-) and promote the formation of cation-(H) CO_3 -complexes, potentially increasing Δ_{47} of the DIC by a small amount (Hill et al., 2020), a salinity difference of 3 psu appears insufficient to explain the large clumped-isotope offsets at Banyuls. There is, however, an alternative way in which salinity may hinder the achievement of clumped-isotope equilibrium in biocarbonates. Increased salinity has been reported to reduce the activity of Carbonic Anhydrase (CA) enzymes both in laboratory experiments

(Nielsen and Frieden, 1972a; Olsen et al., 2022) and in bivalves (Nielsen and Frieden, 1972b). CAs are metalloenzymes, ubiquitous in all metazoans, which increase the rates of CO_2 hydration and HCO_3^- dehydration reactions, promoting isotopic equilibrium within the DIC pool (e.g., Uchikawa and Zeebe, 2012; Watkins and Hunt, 2015; Thaler et al., 2017). Given the time needed to reach isotopic equilibrium without CA (on the order of 1 day or longer Zeebe and Wolf-Gladrow, 2001; Rollion-Bard et al., 2011), the undetectable Δ_{47} departure from equilibrium values at Roscoff supports the assumption that CA is present in bryozoans, as in many other calcifiers. Based on the experimental predictions of Nielsen and Frieden (1972a) and Olsen et al. (2022), we estimate that the increased salinity at Banyuls (~0.59 M [NaCl] vs 0.51 M at Roscoff) could reduce CA activity by 25–35%. A reduction of this magnitude should substantially decrease the rate of isotopes exchange between DIC and water, which is the main process driving DIC species toward isotopic equilibrium. All current models of the evolution of DIC isotopologues predict strong enrichments in Δ_{63} in the early stage following rapid CO_2 absorption (Guo, 2020; Uchikawa et al., 2021; Watkins and Devriendt, 2022). In view of these results, we tentatively propose that increased salinity and the resulting reduction of CA activity is the most likely explanation for the out-of-equilibrium clumped-isotope signatures at Banyuls. We acknowledge that this process alone is not sufficient to explain the $\delta^{18}\text{O}_{\text{w-c}}$ values we observe at both sites, which probably reflects additional fractionations between DIC and the mineral phases (e.g., Watkins et al., 2013; Devriendt et al., 2017).

6. Conclusions

Few studies have attempted so far to reconstruct climate from bryozoan $\delta^{18}\text{O}$ and $\delta^{13}\text{C}$ records due to their polycrystalline patterns and the uncertainty of the potential isotopic disequilibrium issues. Here, we show that combined information from mineralogical and clumped-isotope composition of bryozoan skeleton discriminates between mineralogical, environmental and biological effects and provides keys for a better interpretation.

Our combined $\delta^{18}\text{O}$ and $\delta^{13}\text{C}$ results clearly indicate that bryozoan isotopic composition is controlled by multiple biotic and abiotic factors, potentially hindering their use as paleoenvironmental tracers. Furthermore, our findings document important variations in $\delta^{18}\text{O}$ fractionation between water and carbonate at the scale of a single colony, which cannot simply be attributed to inter-annual temperature variability. These discrepancies might result instead from bryozoan skeleton physiologically controlled resorption/precipitation processes.

This exploratory investigation of bryozoan clumped-isotope highlights potential small mineralogical effects on Δ_{47} and suggests that the Δ_{47} thermometry should be corrected for mineralogy. We also find evidence of >0.02% Δ_{47} offsets from equilibrium, only detectable in samples from the Mediterranean Sea. The existence of these large offsets is likely driven by environmental factors, and we propose that they reflect a salinity-driven decrease in carbonic anhydrase activity. New models accounting for the effect of salinity and other environmental parameters on CA activity are needed to quantitatively estimate the corresponding impact on oxygen and clumped-isotope compositions of bryozoans.

Historically, “vital effects” in carbonates produced by very different organisms have often been described and conceptualized in different ways. Species-specific oxygen-18 fractionation laws in foraminifera were once (and may still be) an indispensable tool for paleoceanographic reconstructions (cf Daeron and Gray, 2023, and references therein), although the influence of seawater chemistry and other parameters has been a growing concern for some time (Spero, 1992; Spero et al., 1997; Spero and Lea, 1993; Zeebe et al., 2008). Isotopic disequilibria in coccolithophores, on the other hand, are best understood using more quantitative models accounting for pCO_2 and other chemical parameters (Rickaby et al., 2010; Hermoso et al., 2016; McClelland et al., 2017), with the magnitude of coccolith disequilibrium effects

having varied substantially at geological time scales (Bolton and Stoll, 2013; Godbillot et al., 2022). In other organisms such as bivalves and cephalopods, ontogenetic processes may strongly modulate ^{13}C , ^{18}O and clumped-isotope signatures (Lorrain et al., 2004; Davies et al., 2021; Huyghe et al., 2020; Huyghe et al., 2022). Our results suggest that, in the case of bryozoans, “vital effects” are not primarily species-specific, but rather a combination of environment-specific and mineralogy-specific, which may be disentangled by pairing isotopic measurements with careful mineralogical characterizations and by comparing bryozoans from different localities.

CRediT authorship contribution statement

Marie Pesnin: Writing – review & editing, Writing – original draft, Methodology, Investigation, Data curation. **Caroline Thaler:** Writing – review & editing, Methodology, Data curation. **Mathieu Daëron:** Writing – review & editing, Supervision, Methodology, Funding acquisition, Data curation. **Sébastien Nomade:** Writing – review & editing, Supervision, Funding acquisition. **Claire Rollion-Bard:** Writing – review & editing, Supervision, Funding acquisition.

Declaration of competing interest

The authors declare that they have no known competing financial interests or personal relationships that could have appeared to influence the work reported in this paper.

Data availability

I have shared the link to my data at the Attach File step

Acknowledgements

We would like to thank Laurent Lévèque and the Service Mer et Plongée of the FR2424/Station Biologique de Roscoff for the logistic support during the sampling. We also acknowledge Yves Plusquellec, Jacques Grall and Franck Lartaud for collecting and providing the rest of the samples. We are also grateful to Sophie Nowak for her help in acquiring and processing the XRD data required for this study. This study has benefited from the instruments through the X-ray facility (Université de Paris, Paris, France) and PARI platform (IPGP, Paris, France) for elemental characterization. This work benefited from the support of the project B2SeaCarb ANR-16-92CE-0010 of the French National Research Agency (ANR). This work was supported by the Paris Ile-de-France Region – DIM “Patrimoines matériels – innovation, expérimentation et résilience” through the project POLIMO. Clumped-isotope facilities (a part of the PANOPLY analytical Platform) at LSCE received funding from various sources (Région Ile-de-France; Commissariat à l’Energie Atomique; Institut National des Sciences de l’Univers/Centre National de la Recherche). This work was supported by a PhD fellowship from CEA (Commissariat à l’Energie Atomique). Thoughtful comments by Editor V. Mavromatis, and three anonymous reviewers helped to improve the original version of the manuscript.

Appendix A. Supplementary data

Supplementary data to this article can be found online at <https://doi.org/10.1016/j.chemgeo.2024.122148>.

References

- Adkins, J.F., Boyle, E.A., Curry, W.B., Lutringer, A., 2003. Stable isotopes in deep-sea corals and a new mechanism for “vital effects”. *Geochim. Cosmochim. Acta* 67 (6), 1129–1143.
- Allison, N., Finch, A.A., 2010. $\delta^{11}\text{B}$, Sr, Mg and B in a modern *Porites* coral: the relationship between calcification site pH and skeletal chemistry. *Geochim. Cosmochim. Acta* 74 (6), 1790–1800.
- Amui-Vedel, A.M., Hayward, P.J., Porter, J.S., 2007. Zooid size and growth rate of the bryozoan *Cryptosula pallasiana* Moll in relation to temperature, in culture and in its natural environment. *J. Exp. Mar. Biol. Ecol.* 353 (1), 1–12.
- Anderson, T.F., Arthur, M.A., 1983. Stable isotopes of oxygen and carbon and their application to sedimentologic and paleoenvironmental problems. *Stable Isotopes in Sedimentary Geology*, Michael a. Arthur, Thomas F. Anderson, Isaac R. Kaplan, Jan Veizer, Lynton S. Land.
- Anderson, N.T., Kelson, J.R., Kele, S., Daëron, M., Bonifacie, M., Horita, J., Bergmann, K. D., 2021. A unified clumped isotope thermometer calibration (0.5–1,100°C) using carbonate-based standardization. *Geophys. Res. Lett.* 48 (7) e2020GL092069.
- Auclair, A.C., Joachimski, M.M., Lécuyer, C., 2003. Deciphering kinetic, metabolic and environmental controls on stable isotope fractionations between seawater and the shell of *Terebratulina transversa* (Brachiopoda). *Chem. Geol.* 202 (1–2), 59–78.
- Bader, B., Schäfer, P., 2005. Impact of environmental seasonality on stable isotope composition of skeletons of the temperate bryozoan *Cellaria sinuosa*. *Palaeogeogr. Palaeoclimatol. Palaeoecol.* 226 (1–2), 58–71.
- Bajnai, D., Fiebig, J., Tomasovych, A., Milner Garcia, S., Rollion-Bard, C., Raddatz, J., Brand, U., 2018. Assessing kinetic fractionation in brachiopod calcite using clumped isotopes. *Sci. Rep.* 8 (1), 533.
- Bajnai, D., Guo, W., Spötl, C., Coplen, T.B., Methner, K., Löffler, N., Fiebig, J., 2020. Dual clumped isotope thermometry resolves kinetic biases in carbonate formation temperatures. *Nat. Commun.* 11 (1), 4005.
- Batson, P.B., Tamberg, Y., Taylor, P.D., Gordon, D.P., Smith, A.M., 2020. Skeletal resorption in bryozoans: occurrence, function and recognition. *Biol. Rev.* 95 (5), 1341–1371.
- Bernasconi, S.M., Müller, I.A., Bergmann, K.D., Breitenbach, S.F., Fernandez, A., Hodell, D.A., Ziegler, M., 2018. Reducing uncertainties in carbonate clumped isotope analysis through consistent carbonate-based standardization. *Geochem. Geophys. Geosyst.* 19 (9), 2895–2914.
- Bernasconi, S.M., Daëron, M., Bergmann, K.D., Bonifacie, M., Meckler, A.N., Affek, H.P., Ziegler, M., 2021. InterCarb: a community effort to improve interlaboratory standardization of the carbonate clumped isotope thermometer using carbonate standards. *Geochem. Geophys. Geosyst.* 22 (5) e2020GC009588.
- Berning, B., Moissette, P., Betzler, C., 2005. Late Miocene Bryozoa from the Guadalquivir Basin (SW Spain): eastern Atlantic and western Mediterranean environment and biogeography. In: *Bryozoan Studies 2004-Proc. 13th Intern. Bryozool. Ass. Conference*, pp. 15–24.
- Blamart, D., Rollion-Bard, C., Cuif, J.P., Juillet-Leclerc, A., Lutringer, A., van Weering, T. C., Henriet, J.P., 2005. C and O isotopes in a deep-sea coral (*Lophelia pertusa*) related to skeletal microstructure. *Cold-water corals and ecosystems*, pp. 1005–1020.
- Blamart, D., Rollion-Bard, C., Meibom, A., Cuif, J.P., Juillet-Leclerc, A., Dauphin, Y., 2007. Correlation of boron isotopic composition with ultrastructure in the deep-sea coral *Lophelia pertusa*: Implications for biomineralization and paleo-pH. *Geochem. Geophys. Geosyst.* 8 (12).
- Boiseau, M., Juillet-Leclerc, A., 1997. H_2O_2 treatment of recent coral aragonite: oxygen and carbon isotopic implications. *Chem. Geol.* 143 (3–4), 171–180.
- Bolton, C.T., Stoll, H.M., 2013. Late Miocene threshold response of marine algae to carbon dioxide limitation. *Nature* 500 (7464), 558–562.
- Bone, Y., James, N.P., 1997. Bryozoan stable isotope survey from the cool-water Lapede Shelf, Southern Australia. *SPEM Special Publication* 56, 93–105.
- Brand, W.A., Assonov, S.S., Coplen, T.B., 2010. Correction for the ^{17}O interference in $\delta^{13}\text{C}$ measurements when analyzing CO_2 with stable isotope mass spectrometry (IUPAC Technical Report). *Pure Appl. Chem.* 82 (8), 1719–1733.
- Brey, T., Gerdes, D., Gutt, J., Mackensen, A., Starmans, A., 1999. Growth and age of the Antarctic bryozoan *Cellaria incula* on the Weddell Sea shelf. *Antarct. Sci.* 11 (4), 408–414.
- Chen, S., Gagnon, A.C., Adkins, J.F., 2018. Carbonic anhydrase, coral calcification and a new model of stable isotope vital effects. *Geochim. Cosmochim. Acta* 236, 179–197.
- Chung, M.T., Chen, C.Y., Shiao, J.C., Shirai, K., Wang, C.H., 2021. Metabolic proxy for cephalopods: Stable carbon isotope values recorded in different biogenic carbonates. *Methods Ecol. Evol.* 12 (9), 1648–1657.
- Cocito, S., Ferdeghini, F., 2001. Carbonate standing stock and carbonate production of the bryozoan *Pentapora fascialis* in the North-Western Mediterranean. *Facies* 45 (1), 25–30.
- Cocito, S., Sgorbini, S., Bianchi, C.N., 1998. Aspects of the biology of the bryozoan *Pentapora fascialis* in the northwestern Mediterranean. *Mar. Biol.* 131 (1), 73–82.
- Coplen, T.B., 2007. Calibration of the calcite–water oxygen-isotope geothermometer at Devil’s Hole, Nevada, a natural laboratory. *Geochim. Cosmochim. Acta* 71 (16), 3948–3957.
- Crowley, S.F., Taylor, P.D., 2000. Stable isotope composition of modern bryozoan skeletal carbonate from the Otago Shelf, New Zealand. *N. Z. J. Mar. Freshw. Res.* 34 (2), 331–352.
- Daëron, M., 2021. Full propagation of analytical uncertainties in Δ_{47} measurements. *Geochim. Geophys. Geosyst.* 22 (5) e2020GC009592.
- Daëron, M., Gray, W.R., 2023. Revisiting oxygen-18 and clumped isotopes in planktic and benthic foraminifera. *Paleoceanography and Paleoclimatology* 38 (10) e2023PA004660.
- Daëron, M., Vermeesch, P., 2024. Omnidirectional Generalized Least Squares Regression: Theory, Geochronological applications, and making the Case for Reconciled Δ_{47} Calibrations. *Chem* 647, 121881.
- Daëron, M., Blamart, D., Peral, M., Affek, H.P., 2016. Absolute isotopic abundance ratios and the accuracy of Δ_{47} measurements. *Chem. Geol.* 442, 83–96.
- Daëron, M., Drysdale, R.N., Peral, M., Huyghe, D., Blamart, D., Coplen, T.B., Zanchetta, G., 2019. Most Earth-surface calcites precipitate out of isotopic equilibrium. *Nat. Commun.* 10 (1), 429.

- Davies, A.J., John, C.M., 2019. The clumped ($^{13}\text{C}^{18}\text{O}$) isotope composition of echinoid calcite: further evidence for “vital effects” in the clumped isotope proxy. *Geochim. Cosmochim. Acta* 245, 172–189.
- Davies, A.J., Davis, S., John, C.M., 2021. Evidence of taxonomic non-equilibrium effects in the clumped isotope composition of modern cephalopod carbonate. *Chem. Geol.* 578, 120317.
- Davies, A.J., Guo, W., Bernecker, M., Tagliavento, M., Raddatz, J., Gischler, E., et al., 2022. Dual clumped isotope thermometry of coral carbonate. *Geochim. Cosmochim. Acta* 338, 66–78.
- Davies, A.J., Brand, U., Tagliavento, M., Bitner, M.A., Bajnai, D., Staudigel, P., et al., 2023. Isotopic disequilibrium in brachiopods disentangled with dual clumped isotope thermometry. *Geochim. Cosmochim. Acta* 359, 135–147.
- De Winter, N.J., Witbaard, R., Kocken, I.J., Müller, I.A., Guo, J., Goudsmit, B., Ziegler, M., 2022. Temperature dependence of clumped isotopes (Δ_{47}) in aragonite. *Geophys. Res. Lett.* 49 (20) e2022GL099479.
- Devriendt, L.S., Watkins, J.M., McGregor, H.V., 2017. Oxygen isotope fractionation in the $\text{CaCO}_3\text{-DIC-H}_2\text{O}$ system. *Geochim. Cosmochim. Acta* 214, 115–142.
- Dong, J., Eiler, J., An, Z., Li, X., Lui, W., 2021. Clumped isotopic composition of cultured and natural land-snail shells and their implications. *Palaeogeogr. Palaeoclimatol. Palaeoecol.* 577, 110530.
- Eiler, J.M., Schauble, E., 2004. $^{18}\text{O}^{13}\text{C}^{16}\text{O}$ in Earth’s atmosphere. *Geochim. Cosmochim. Acta* 68 (23), 4767–4777.
- Epstein, S., Buchsbaum, R., Lowenstam, H.A., Urey, H.C., 1953. Revised carbonate-water isotopic temperature scale. *Geol. Soc. Am. Bull.* 64 (11), 1315–1326.
- Erz, J., 2003. The source of ions for biomineralization in foraminifera and their implications for paleoceanographic proxies. *Rev. Mineral. Geochem.* 54 (1), 115–149.
- Fiebig, J., Daëron, M., Bernecker, M., Guo, W., Schneider, G., Boch, R., et al., 2021. Calibration of the dual clumped isotope thermometer for carbonates. *Geochim. Cosmochim. Acta* 312, 235–256.
- Figueroa, B., Griffiths, H.J., Krzeminska, M., Piwoni-Piorewicz, A., Iglikowska, A., Kuklinski, P., 2023. Temperature as a likely driver shaping global patterns in mineralogical composition in bryozoans: implications for marine calcifiers under global change. *Ecography* 2023 (1), e06381.
- Forester, R.M., Sandberg, P.A., Anderson, T.F., 1973. Isotopic variability of cheilostome bryozoan skeletons. In: Larwood, G.P. (Ed.), *Living and Fossil bryozoa*. Academic Press, London, pp. 79–94.
- Fortunato, H., 2015. Bryozoans in climate and ocean acidification research: a reappraisal of an under-used tool. *Reg. Stud. Mar. Sci.* 2, 32–44.
- Furla, P., Allemand, D., Orsenigo, M.N., 2000. Involvement of H^+ -ATPase and carbonic anhydrase in inorganic carbon uptake for endosymbiont photosynthesis. *Am. J. Phys. Regul. Integr. Comp. Phys.* 278 (4), R870–R881.
- Gabitov, R.I., Watson, E.B., Sadekov, A., 2012. Oxygen isotope fractionation between calcite and fluid as a function of growth rate and temperature: an *in situ* study. *Chem. Geol.* 306, 92–102.
- Ghosh, P., Adkins, J., Afeek, H., Balta, B., Guo, W., Schauble, E.A., et al., 2006. $^{13}\text{C}-^{18}\text{O}$ bonds in carbonate minerals: a new kind of paleothermometer. *Geochim. Cosmochim. Acta* 70 (6), 1439–1456.
- Godbillon, C., Minoletti, F., Bassinot, F., Hermoso, M., 2022. Parallel between the isotopic composition of coccolith calcite and carbon levels across termination II: developing a new paleo- CO_2 probe. *Clim. Past* 18 (3), 449–464.
- Goodwin, D.H., Schone, B.R., Dettman, D.L., 2003. Resolution and fidelity of oxygen isotopes as paleotemperature proxies in bivalve mollusk shells: models and observations. *Palaeos* 18 (2), 110–125.
- Gray, W.R., Evans, D., Henehan, M., Weldeab, S., Lea, D.W., Müller, W., Rosenthal, Y., 2023. Sodium incorporation in foraminiferal calcite: an evaluation of the Na/ca salinity proxy and evidence for multiple Na-bearing phases. *Geochim. Cosmochim. Acta* 348, 152–164.
- Grossman, E.L., Ku, T.L., 1986. Oxygen and carbon isotope fractionation in biogenic aragonite: temperature effects. *Chemical Geology: Isotope Geoscience Section* 59, 59–74.
- Grottoli, A.G., Rodrigues, L.J., Matthews, K.A., Palardy, J.E., Gibb, O.T., 2005. Pre-treatment effects on coral skeletal $\delta^{13}\text{C}$ and $\delta^{18}\text{O}$. *Chem. Geol.* 221 (3–4), 225–242.
- Guo, W., 2008. Carbonate Clumped Isotope Thermometry: Application to Carbonaceous Chondrites & Effects of Kinetic Isotope Fractionation. PhD thesis.. California Institute of Technology.
- Guo, W., 2020. Kinetic clumped isotope fractionation in the $\text{DIC-H}_2\text{O-CO}_2$ system: patterns, controls, and implications. *Geochim. Cosmochim. Acta* 268, 230–257.
- Hageman, S.J., Needham, L.L., Todd, C.D., 2009. Threshold effects of food concentration on the skeletal morphology of the bryozoan *Electra pilosa* (Linnaeus, 1767). *Lethaia* 42 (4), 438–451.
- Håkansson, E., Madsen, L., 1991. Symbiosis—a plausible explanation of gigantism in Permian trepostome bryozoans. In: Bigey, F.P., d’Hondt, J.-L. (Eds.), *Bryozoaires Actuels et Fossiles. Bulletin Société de Sciences National de l’Ouest de la France Memoir*, Nantes, pp. 151–159.
- Hemming, N.G., Hanson, G.N., 1992. Boron isotopic composition and concentration in modern marine carbonates. *Geochim. Cosmochim. Acta* 56 (1), 537–543.
- Henkes, G.A., Passey, B.H., Wanamaker Jr., A.D., Grossman, E.L., Ambrose Jr., W.G., Carroll, M.L., 2013. Carbonate clumped isotope compositions of modern marine mollusk and brachiopod shells. *Geochim. Cosmochim. Acta* 106, 307–325.
- Hermoso, M., Chan, I.Z.X., McClelland, H.L.O., Heureux, A.M.C., Rickaby, R.E.M., 2016. Vanishing coccolith vital effects with alleviated carbon limitation. *Biogeosciences* 13 (1), 301–312.
- Hill, P.S., Tripati, A.K., Schauble, E.A., 2014. Theoretical constraints on the effects of pH, salinity, and temperature on clumped isotope signatures of dissolved inorganic carbon species and precipitating carbonate minerals. *Geochim. Cosmochim. Acta* 125, 610–652.
- Hill, P.S., Schauble, E.A., Tripati, A., 2020. Theoretical constraints on the effects of added cations on clumped oxygen, and carbon isotope signatures of dissolved inorganic carbon species and minerals. *Geochim. Cosmochim. Acta* 269, 496–539.
- Huyghe, D., Daëron, M., de Rafélis, Blamart, D., Sébilo, M., Paulet, M.Y., Lartaud, F., 2022. Clumped isotopes in modern marine bivalves. *Geochim. Cosmochim. Acta* 316, 41–58.
- Huyghe, D., Emmanuel, L., de Rafélis, M., Renard, M., Ropert, M., Labourdette, N., Lartaud, F., 2020. Oxygen isotope disequilibrium in the juvenile portion of oyster shells biases seawater temperature reconstructions. *Estuar. Coast. Shelf Sci.* 240, 106777.
- Jackson, J.B.C., Herrera-Cubilla, A., 2000. Adaptation and Constraint as Determinants of Zoid and Ovicell Size among Encrusting Ascophoran Cheilostome Bryozoa from Opposite Sides of the Isthmus of Panama. In: Proceedings of the 11th International Bryozoology Association Conference. (Ed. by A. Herrera Cabilla and J.B.C Jackson). Smithsonian Tropical Research Institute, Balboa, Panama, pp. 249–258.
- Jimenez-Lopez, C., Romanek, C.S., Huertas, F.J., Ohmoto, H., Caballero, E., 2004. Oxygen isotope fractionation in synthetic magnesian calcite. *Geochim. Cosmochim. Acta* 68 (16), 3367–3377.
- Jimenez-Lopez, C., Romanek, C.S., Caballero, E., 2006. Carbon isotope fractionation in synthetic magnesian calcite. *Geochim. Cosmochim. Acta* 70 (5), 1163–1171.
- Johnson, K.S., 1982. Carbon dioxide hydration and dehydration kinetics in seawater 1. *Limnol. Oceanogr.* 27 (5), 849–855.
- Key Jr., M.M., Wyse Jackson, P.N., Håkansson, E., Patterson, W.P., Moore, M.D., 2005. Gigantism in Permian trepostomes from Greenland: testing the algal symbiosis hypothesis using ^{13}C and ^{18}O values. *Bryozoan studies 2004*, 141–151.
- Key Jr., M.M., Smith, A.M., Phillips, N.J., Forrester, J.S., 2020. Effect of removal of organic material on stable isotope ratios in skeletal carbonate from taxonomic groups with complex mineralogies. *Rapid Commun. Mass Spectrom.* 34 (20), e8901.
- Key, M.M., Zágoršek, K., Patterson, W.P., 2013. Paleoenvironmental reconstruction of the early to Middle Miocene Central Paratethys using stable isotopes from bryozoan skeletons. *Int. J. Earth Sci.* 102, 305–318.
- Kim, S.T., O’Neil, J.R., 1997. Equilibrium and nonequilibrium oxygen isotope effects in synthetic carbonates. *Geochim. Cosmochim. Acta* 61 (16), 3461–3475.
- Kim, S.T., Mucci, A., Taylor, B.E., 2007a. Phosphoric acid fractionation factors for calcite and aragonite between 25 and 75°C: revisited. *Chem. Geol.* 246 (3–4), 135–146.
- Kim, S.T., O’Neil, J.R., Hillaire-Marcel, C., Mucci, A., 2007b. Oxygen isotope fractionation between synthetic aragonite and water: Influence of temperature and Mg^{2+} concentration. *Geochim. Cosmochim. Acta* 71 (19), 4704–4715.
- Kimball, J., Eagle, R., Dunbar, R., 2016. Carbonate “clumped” isotope signatures in aragonitic scleractinian and calcitic gorgonian deep-sea corals. *Biogeosciences* 13 (23), 6487–6505.
- Knowles, T., Taylor, P.D., Williams, M., Haywood, A.M., Okamura, B., 2009. Pliocene seasonality across the North Atlantic inferred from cheilostome bryozoans. *Palaeogeogr. Palaeoclimatol. Palaeoecol.* 277 (3–4), 226–235.
- Knowles, T., Leng, M.J., Williams, M., Taylor, P.D., Sloane, H.J., Okamura, B., 2010. Interpreting seawater temperature range using oxygen isotopes and zooid size variation in *Pentapora foliacea* (Bryozoa). *Mar. Biol.* 157, 1171–1180.
- Lartaud, F., Emmanuel, L., De Rafélis, M., Ropert, M., Labourdette, N., Richardson, C.A., Renard, M., 2010. A latitudinal gradient of seasonal temperature variation recorded in oyster shells from the coastal waters of France and the Netherlands. *Facies* 56, 13–25.
- Lebeau, O., Busigny, V., Chaduteau, C., Ader, M., 2014. Organic matter removal for the analysis of carbon and oxygen isotope compositions of siderite. *Chem. Geol.* 372, 54–61.
- LeGrande, A.N., Schmidt, G.A., 2006. Global gridded data set of the oxygen isotopic composition in seawater. *Geophys. Res. Lett.* 33, L12604.
- Letulle, T., Gaspard, D., Daëron, M., Arnaud-Godet, F., Vinçon-Lauzier, A., Suan, G., Lécuyer, C., 2023. Multi-proxy assessment of brachiopod shell calcite as a potential archive of seawater temperature and oxygen isotope composition. *Biogeosciences* 20 (7), 1381–1403.
- Levit, N.P., Eiler, J.M., Romanek, C.S., Beard, B.L., Xu, H., Johnson, C.M., 2018. Near Equilibrium $^{13}\text{C}-^{18}\text{O}$ Bonding during Inorganic Calcite Precipitation under Chemo-Stat Conditions. *Geochem. Geophys. Geosyst.* 19 (3), 901–920.
- Liu, B., Six, K.D., Ilyina, T., 2021. Incorporating the stable carbon isotope ^{13}C in the ocean biogeochemical component of the Max Planck Institute Earth System Model. *Biogeosciences* 18 (14), 4389–4429.
- Lombardi, C., Cocito, S., Hiscock, K., Occhipinti-Ambrogi, A., Setti, M., Taylor, P.D., 2008. Influence of seawater temperature on growth bands, mineralogy and carbonate production in a bioconstructional bryozoan. *Facies* 54, 333–342.
- Lorrain, A., Paulet, Y.M., Chauvaud, L., Dunbar, R., Mucciarone, D., Fontugne, M., 2004. $\delta^{13}\text{C}$ variation in scallop shells: increasing metabolic carbon contribution with body size? *Geochim. Cosmochim. Acta* 68 (17), 3509–3519.
- Loxton, J., Kuklinski, P., Najorka, J., Jones, M.S., Porter, J.S., 2014. Variability in the skeletal mineralogy of temperate bryozoans: the relative influence of environmental and biological factors. *Mar. Ecol. Prog. Ser.* 510, 45–57.
- Loxton, J., Najorka, J., Humphreys-Williams, E., Kuklinski, P., Smith, A.M., Porter, J.S., Jones, M.S., 2017. The forgotten variable: Impact of cleaning on the skeletal composition of a marine invertebrate. *Chem. Geol.* 474, 45–57.
- Lutterotti, L., Chateigner, D., Ferrari, S., Ricote, J., 2004. Texture, residual stress and structural analysis of thin films using a combined X-ray analysis. *Thin Solid Films* 450, 34–41.
- Machiya, H., Yamada, T., Kaneko, N., Iryu, Y., Odawara, K., Asami, R., James, N.P., 2003. Carbon and oxygen isotopes of cool-water bryozoans from the Great

- Australian Bight and their paleoenvironmental significance. Proceedings of the Ocean Drilling Programme, Scientific Results 182, 1–29.
- Marchegiano, M., Peral, M., Venderickx, J., Martens, K., García-Alix, A., Snoeck, C., Claeys, P., 2024. The ostracod clumped-isotope thermometer: a novel tool to accurately quantify continental climate changes. *Geophys. Res. Lett.* 51 (4) e2023GL107426.
- Mavromatis, V., Schmidt, M., Botz, R., Comas-Bru, L., Oelkers, E.H., 2012. Experimental quantification of the effect of Mg on calcite-aqueous fluid oxygen isotope fractionation. *Chem. Geol.* 310, 97–105.
- McClelland, H.L.O., Bruggeman, J., Hermoso, M., Rickaby, R.E.M., 2017. The origin of carbon isotope vital effects in coccolith calcite. *Nat. Commun.* 8 (1), 14511.
- McConaughey, T., 1989a. ^{13}C and ^{18}O isotopic disequilibrium in biological carbonates: I. Patterns. *Geochim. Cosmochim. Acta* 53 (1), 151–162.
- McConaughey, T., 1989b. ^{13}C and ^{18}O isotopic disequilibrium in biological carbonates: II. In vitro simulation of kinetic isotope effects. *Geochim. Cosmochim. Acta* 53 (1), 163–171.
- McCulloch, M., Falter, J., Trotter, J., Montagna, P., 2012. Coral resilience to ocean acidification and global warming through pH up-regulation. *Nat. Clim. Chang.* 2 (8), 623–627.
- Meinicke, N., Ho, S.L., Hannisdal, B., Nürnberg, D., Tripathi, A., Schiebel, R., Meckler, A.N., 2020. A robust calibration of the clumped isotopes to temperature relationship for foraminifers. *Geochim. Cosmochim. Acta* 270, 160–183.
- Nehyba, S., Tománová-Petrová, P., Zágorsek, K., 2008. Sedimentological and palaeoecological records of the evolution of the southwestern part of the Carpathian Foredeep (Czech Republic) during the early Badenian. *Geological Quarterly* 52 (1), 45–60.
- Nielsen, S.A., Frieden, E., 1972a. Some chemical and kinetic properties of oyster carbonic anhydrase. *Comp. Biochem. and Physiol. Part B: Comp. Biochem.* 41 (4), 875–889.
- Nielsen, S.A., Frieden, E., 1972b. Carbonic anhydrase activity in molluscs. *Comp. Biochem. and Physiol. Part B: Comp. Biochem.* 41 (3), 461–468.
- Novosel, M., Požar-Domac, A., Pasarić, M., 2004. Diversity and distribution of the Bryozoa along underwater cliffs in the Adriatic Sea with special reference to thermal regime. *Mar. Ecol.* 25 (2), 155–170.
- O'Dea, A., 2003. Seasonality and zooid size variation in Panamanian encrusting bryozoans. *J. Mar. Biol. Assoc. UK* 83, 1107–1108.
- Olsen, E.K., Watkins, J.M., Devriendt, L.S., 2022. Oxygen isotopes of calcite precipitated at high ionic strength: CaCO_3 -DIC fractionation and carbonic anhydrase inhibition. *Geochim. Cosmochim. Acta* 325, 170–186.
- Parkinson, D., Curry, G.B., Cusack, M., Fallick, A.E., 2005. Shell structure, patterns and trends of oxygen and carbon stable isotopes in modern brachiopod shells. *Chem. Geol.* 219 (1–4), 193–235.
- Pätzold, J., Ristedt, H., Wefer, G., 1987. Rate of growth and longevity of a large colony of *Pentapora foliacea* (Bryozoa) recorded in their oxygen isotope profiles. *Mar. Biol.* 96, 535–538.
- Peral, M., Daëron, M., Blamart, D., Bassinot, F., Dewilde, F., Smialkowski, N., et al., 2018. Updated calibration of the clumped isotope thermometer in planktonic and benthic foraminifera. *Geochim. Cosmochim. Acta* 239, 1–16.
- Petersen, S.V., Deflise, W.F., Saenger, C., Daëron, M., Huntington, K.W., John, C.M., Winkelstern, I.Z., 2019. Effects of improved ^{17}O correction on interlaboratory agreement in clumped isotope calibrations, estimates of mineral-specific offsets, and temperature dependence of acid digestion fractionation. *Geochem. Geophys. Geosyst.* 20 (7), 3495–3519.
- Pierre, C., 1999. The oxygen and carbon isotope distribution in the Mediterranean water masses. *Mar. Geol.* 153 (1–4), 41–55.
- Rao, C.P., Nelson, C.S., 1992. Oxygen and carbon isotope fields for temperate shelf carbonates from Tasmania and New Zealand. *Mar. Geol.* 103 (1–3), 273–286.
- Rickaby, R.E., Henderiks, J., Young, J.N., 2010. Perturbing phytoplankton: response and isotopic fractionation with changing carbonate chemistry in two coccolithophore species. *Clim. Past* 6 (6), 771–785.
- Rollion-Bard, C., Erez, J., 2010. Intra-shell boron isotope ratios in the symbiont-bearing benthic foraminiferan *Amphistegina lobifera*: Implications for ^{8}B vital effects and paleo-pH reconstructions. *Geochim. Cosmochim. Acta* 74 (5), 1530–1536.
- Rollion-Bard, C., Blamart, D., Cuif, J.P., Juillet-Leclerc, A., 2003a. Microanalysis of C and O isotopes of azooxanthellate and zooxanthellate corals by ion microprobe. *Coral Reefs* 22, 405–415.
- Rollion-Bard, C., Chaussidon, M., France-Lanord, C., 2003b. pH control on oxygen isotopic composition of symbiotic corals. *Earth Planet. Sci. Lett.* 215 (1–2), 275–288.
- Rollion-Bard, C., Blamart, D., Cuif, J.P., Dauphin, Y., 2010. In situ measurements of oxygen isotopic composition in deep-sea coral, *Lophelia pertusa*: Re-examination of the current geochemical models of biomineralization. *Geochim. Cosmochim. Acta* 74 (4), 1338–1349.
- Rollion-Bard, C., Chaussidon, M., France-Lanord, C., 2011. Biological control of internal pH in scleractinian corals: Implications on paleo-pH and paleo-temperature reconstructions. *Compt. Rendus Geosci.* 343 (6), 397–405.
- Rollion-Bard, C., Saulnier, S., Vigier, N., Schumacher, A., Chaussidon, M., Lécuyer, C., 2016. Variability in magnesium, carbon and oxygen isotope compositions of brachiopod shells: implications for paleoceanographic studies. *Chem. Geol.* 423, 49–60.
- Romanek, C.S., Grossman, E.L., Morse, J.W., 1992. Carbon isotopic fractionation in synthetic aragonite and calcite: effects of temperature and precipitation rate. *Geochim. Cosmochim. Acta* 56 (1), 419–430.
- Ryland, J.S., Sykes, A.M., 1972. The analysis of pattern in communities of bryozoa. I. Discrete sampling methods. *J. Exp. Mar. Biol. Ecol.* 8 (3), 277–297.
- Saenger, C., Affek, H.P., Felis, T., Thiagarajan, N., Lough, J.M., Holcomb, M., 2012. Carbonate clumped isotope variability in shallow water corals: Temperature dependence and growth-related vital effects. *Geochim. Cosmochim. Acta* 99, 224–242.
- Schauble, E.A., Ghosh, P., Eiler, J.M., 2006. Preferential formation of ^{13}C - ^{18}O bonds in carbonate minerals, estimated using first-principles lattice dynamics. *Geochim. Cosmochim. Acta* 70 (10), 2510–2529.
- Smith, A.M., 2014. Growth and calcification of marine bryozoans in a changing ocean. *Biol. Bull.* 226 (3), 203–210.
- Smith, A.M., Key, M.M., 2004. Controls, variation, and a record of climate change in detailed stable isotope record in a single bryozoan skeleton. *Quat. Res.* 61 (2), 123–133.
- Smith, J.E., Schwarcz, H.P., Risk, M.J., McConaughey, T.A., Keller, N., 2000. Paleotemperatures from deep-sea corals: overcoming 'vital effects'. *Palaios* 15 (1), 25–32.
- Smith, A.M., Stewart, B., Key, M.M., Jamet, C.M., 2001. Growth and carbonate production by *Adeonellopsis* (Bryozoa Cheilostomata) in Doubtful Sound, New Zealand. *Palaeogeogr. Palaeoclimatol. Palaeoecol.* 175, 201–210.
- Smith, A.M., Nelson, C.S., Key, M.M., Patterson, W.P., 2004. Stable isotope values in modern bryozoan carbonate from New Zealand and implications for paleoenvironmental interpretation. *N. Z. J. Geol. Geophys.* 47 (4), 809–821.
- Smith, A.M., Key Jr., M.M., Gordon, D.P., 2006. Skeletal mineralogy of bryozoans: taxonomic and temporal patterns. *Earth Sci. Rev.* 78 (3–4), 287–306.
- Spero, H.J., 1992. Do planktic foraminifera accurately record shifts in the carbon isotopic composition of seawater ΣCO_2 ? *Mar. Micropaleontol.* 19 (4), 275–285.
- Spero, H.J., Lea, D.W., 1993. Intrasppecific stable isotope variability in the planktic foraminifera *Globigerinoides sacculifer*: results from laboratory experiments. *Mar. Micropaleontol.* 22 (3), 221–234.
- Spero, H.J., Lea, D.W., 1996. Experimental determination of stable isotope variability in *Globigerina bulloides*: Implications for paleoceanographic reconstructions. *Mar. Micropaleontol.* 28 (3–4), 231–246.
- Spero, H.J., Bijma, J., Lea, D.W., Bemis, B.E., 1997. Effect of seawater carbonate concentration on foraminiferal carbon and oxygen isotopes. *Nature* 390 (6659), 497–500.
- Spooner, P.T., Guo, W., Robinson, L.F., Thiagarajan, N., Hendry, K.R., Rosenheim, B.E., Leng, M.J., 2016. Clumped isotope composition of cold-water corals: a role for vital effects? *Geochim. Cosmochim. Acta* 179, 123–141.
- Stebbing, A.R.D., 1971. Growth of *Flustra foliacea* (Bryozoa). *Mar. Biol.* 9, 267–273.
- Swezey, D.S., Bean, J.R., Ninokawa, A.T., Hill, T.M., Gaylord, B., Sanford, E., 2017. Interactive effects of temperature, food and skeletal mineralogy mediate biological responses to ocean acidification in a widely distributed bryozoan. *Proc. R. Soc. B Biol. Sci.* 284 (1853), 20162349.
- Tarutani, T., Clayton, R.N., Mayeda, T.K., 1969. The effect of polymorphism and magnesium substitution on oxygen isotope fractionation between calcium carbonate and water. *Geochim. Cosmochim. Acta* 33 (8), 987–996.
- Tavener-Smith, R., Williams, A., 1972. The secretion and structure of the skeleton of living and fossil Bryozoa. *Philosophical Transactions of the Royal Society of London. B Biological Sciences* 264 (859), 97–160.
- Taylor, P.D., Kuklinski, P., 2011. Seawater chemistry and biominerization: did trepostome bryozoans become hypercalcified in the calcite sea of the Ordovician? *Palaeobiodiversity and Palaeoenvironments* 91, 185–195.
- Taylor, P.D., Waeschenbach, A., 2015. Phylogeny and diversification of bryozoans. *Palaeontology* 58 (4), 585–599.
- Taylor, P.D., James, N.P., Bone, Y., Kuklinski, P., Kyser, T.K., 2009. Evolving mineralogy of cheilostome bryozoans. *Palaios* 24 (7), 440–452.
- Taylor, P.D., Vinn, O., Wilson, M.A., 2010. Evolution of biomineralization in 'Lophophorates'. *Spec. Pap. Palaeontol.* 84, 317–333.
- Taylor, P.D., Lombardi, C., Cocito, S., 2015. Biomineralization in bryozoans: present, past and future. *Biol. Rev.* 90 (4), 1118–1150.
- Thaler, C., Millo, C., Ader, M., Chaduteau, C., Guyot, F., Ménez, B., 2017. Disequilibrium $\delta^{18}\text{O}$ values in microbial carbonates as a tracer of metabolic production of dissolved inorganic carbon. *Geochim. Cosmochim. Acta* 199, 112–129.
- Thiagarajan, N., Adkins, J., Eiler, J., 2011. Carbonate clumped isotope thermometry of deep-sea corals and implications for vital effects. *Geochim. Cosmochim. Acta* 75 (16), 4416–4425.
- Tripathi, A.K., Eagle, R.A., Thiagarajan, N., Gagnon, A.C., Bauch, H., Halloran, P.R., Eiler, J.M., 2010. ^{13}C - ^{18}O isotope signatures and 'clumped isotope' thermometry in foraminifera and coccoliths. *Geochim. Cosmochim. Acta* 74 (20), 5697–5717.
- Uchikawa, J., Zeebe, R.E., 2012. The effect of carbonic anhydrase on the kinetics and equilibrium of the oxygen isotope exchange in the CO_2 - H_2O system: Implications for ^{18}O vital effects in biogenic carbonates. *Geochim. Cosmochim. Acta* 95, 15–34.
- Uchikawa, J., Chen, S., Eiler, J.M., Adkins, J.F., Zeebe, R.E., 2021. Trajectory and timescale of oxygen and clumped isotope equilibration in the dissolved carbonate system under normal and enzymatically-catalyzed conditions at 25 °C. *Geochim. Cosmochim. Acta* 314, 313–333.
- Urey, H.C., 1947. The thermodynamic properties of isotopic substances. *J. Chem. Soc. (Resumed)* 562–581.
- Watkins, J.M., Devriendt, L.S., 2022. A combined model for kinetic clumped isotope effects in the CaCO_3 -DIC- H_2O system. *Geochem. Geophys. Geosyst.* 23 (8) e2021GC010200.
- Watkins, J.M., Hunt, J.D., 2015. A process-based model for non-equilibrium clumped isotope effects in carbonates. *Earth Planet. Sci. Lett.* 432, 152–165.
- Watkins, J.M., Nielsen, L.C., Ryerson, F.J., DePaolo, D.J., 2013. The influence of kinetics on the oxygen isotope composition of calcium carbonate. *Earth Planet. Sci. Lett.* 375, 349–360.
- Watkins, J.M., Hunt, J.D., Ryerson, F.J., DePaolo, D.J., 2014. The influence of temperature, pH, and growth rate on the $\delta^{18}\text{O}$ composition of inorganically precipitated calcite. *Earth Planet. Sci. Lett.* 404, 332–343.

- Zeebe, R.E., Wolf-Gladrow, D., 2001. CO₂ in seawater: Equilibrium, kinetics, isotopes. In: Elsevier Oceanography Series, , 1st ed65. Elsevier, Amsterdam.
- Zeebe, R.E., Bijma, J., Hönnisch, B., Sanyal, A., Spero, H.J., Wolf-Gladrow, D.A., 2008. Vital effects and beyond: a modelling perspective on developing palaeoceanographical proxy relationships in foraminifera. *Geol. Soc. Lond. Spec. Publ.* 303 (1), 45–58.
- Zhou, G.T., Zheng, Y.F., 2005. Effect of polymorphic transition on oxygen isotope fractionation between aragonite, calcite and water: a low-temperature experimental study. *Am. Mineral.* 90, 1121–1130.